International Journal of Earth Sciences (2019) 108:1571–1593
https://doi.org/10.1007/s00531-019-01720-y

ORIGINAL PAPER

Provenance and Variscan low-grade regional metamorphism recorded in slates from the basement of the (SW Hungary)

Előd Mészáros[1,2] · Andrea Varga[1] · Béla Raucsik[1] · Zsolt Benkó[2] · Adrián Heincz[1] · Christoph A. Hauzenberger[3]

Received: 9 April 2018 / Accepted: 23 April 2019 / Published online: 4 May 2019
© The Author(s) 2019

Abstract

A metapelitic sequence with Silurian protolith from the Horváthertelend Unit (Tisza Mega-unit, Hungary) has a K-white mica + chlorite + quartz + albite + anatase ± tourmaline mineral assemblage. Moderately developed disjunctive and well-developed continuous foliations are present. Geochemical results reflect a dominantly felsic source of the protoliths, suggesting an intermediate to acidic volcanic arc in the provenance area. Metasandstone pebbles in the metaconglomerate indicate a recycled sedimentary source. Raman spectroscopy of carbonaceous material indicates a ~ 350−370 °C peak metamorphic temperature. The Kübler Index (KI_{Basel}) values of the phengitic K-white mica indicate epizonal metamorphism (0.22 ± 0.04 $\Delta°2\theta$). The Chlorite 'Crystallinity' Index (ChC_{CIS}) suggests metamorphic alteration near to the anchizone−epizone boundary (0.31 ± 0.06 $\Delta°2\theta$). K–Ar ages of K-white mica are interpreted as a result of Variscan metamorphism (*c.* > 310 Ma) and post-Variscan uplift (*c.* 290 Ma). The predominance of lydite and slate of Llandoverian age and the overlying coarse-grained metagreywacke and metaconglomerate beds of the Szalatnak Slate Formation show strong lithological similarities with the proximal Silurian sequences in the Małopolska Massif (Kielce Region, Holy Cross Mountains, Poland). The original position of the Horváthertelend Unit is presumably to the northeast from the Bohemian Massif, next to the Upper Silesian Block (Moravo-Silesian Zone) and the Małopolska Terrane.

Keywords Carbonaceous material · K-white mica · Provenance · Variscan metamorphism · Palaeogeography · Tisza Mega-unit

Introduction

The European Variscan and Alpine mountain chains are collisional orogens and are built up of pre-Variscan basement blocks originated at the Gondwana Palaeo-tethyan margin (von Raumer et al. 2003; Novo-Fernández et al. 2016). Pre-Variscan domains, such as the Iberian Massif, Bohemian Massif and French Massif Central, are essential components in the Variscan basement areas in Western and Central Europe (von Raumer et al. 2003; Kroner et al. 2008). Reconstructions of the Variscan Orogen illustrate a complex evolution with different tectonic units, including a variety of (par) autochthonous sections suffered metamorphism (e.g., Novo-Fernández et al. 2016). The Variscan orogenic phase resulted in superimposed structures and juxtaposition of pre-Variscan and Variscan blocks (von Raumer et al. 2003; Kroner et al. 2008; Kříbek et al. 2009). The Bohemian Massif represents the eastern termination of the European Variscan Orogen. Further Variscan continental crust fragments to the southeast are, however, partly hidden and/or moderately to strongly overprinted by the subsequent Alpine Orogeny (Fig. 1a).

The southern part of the Bohemian Massif belongs to the Moldanubian Zone (sensu stricto) which is a key part of the Variscan Internides (Kroner et al. 2008 and references therein). This internal zone is characterized by individual

Electronic supplementary material The online version of this article (https://doi.org/10.1007/s00531-019-01720-y) contains supplementary material, which is available to authorized users.

✉ Előd Mészáros
meszaros.elod@gmail.com

[1] 'Vulcano' Petrology and Geochemistry Research Group, Department of Mineralogy, Geochemistry and Petrology, University of Szeged, Egyetem utca 2, 6722 Szeged, Hungary

[2] Isotope Climatology and Environmental Research Centre, Institute for Nuclear Research, Hungarian Academy of Sciences, Bem tér 18/c, Debrecen 4026, Hungary

[3] Institute of Earth Science, University of Graz, Universitätsplatz 2., 8010 Graz, Austria

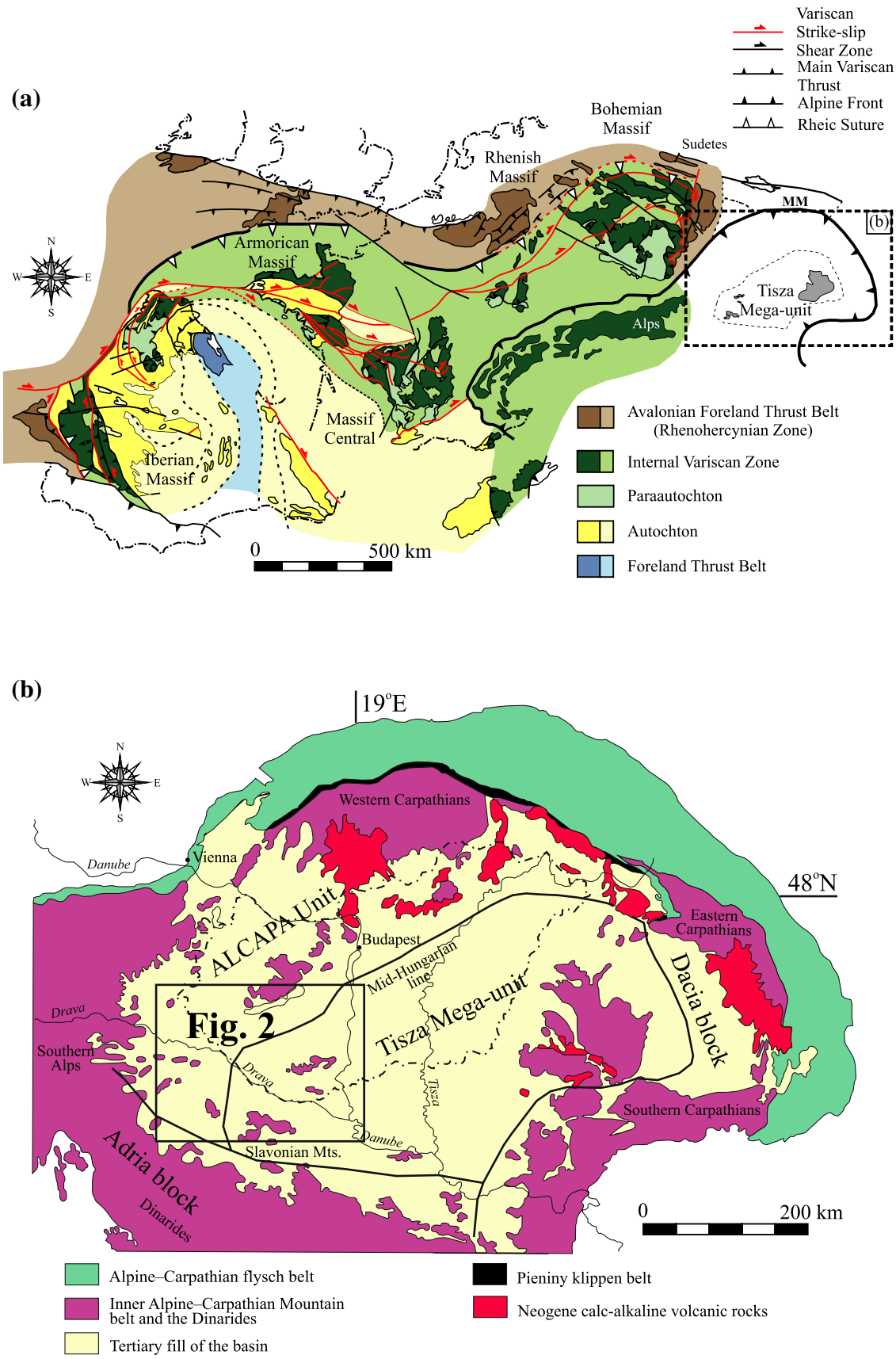
(a)
Variscan
Strike-slip
Shear Zone
Main Variscan
Thrust
Alpine Front
Rheic Suture
Bohemian Massif
Sudetes
Rhenish Massif
MM
(b)
Armorican Massif
Tisza Mega-unit
Alps
Massif Central
Iberian Massif
0
500 km
Avalonian Foreland Thrust Belt (Rhenohercynian Zone)
Internal Variscan Zone
Paraautochton
Autochton
Foreland Thrust Belt
(b)
19°E
48°N
Western Carpathians
Vienna
Danube
ALCAPA Unit
Budapest
Mid-Hungarian line
Eastern Carpathians
Dacia block
Tisza Mega-unit
Fig. 2
Drava
Southern Alps
Drava
Tisza
Danube
Slavonian Mts.
Southern Carpathians
Adria block
Dinarides
0
200 km
Alpine–Carpathian flysch belt
Inner Alpine–Carpathian Mountain belt and the Dinarides
Tertiary fill of the basin
Pieniny klippen belt
Neogene calc-alkaline volcanic rocks

◂**Fig. 1** **a** Structure and zonation of the European Variscan Orogen with indication of the location of Pannonian Basin (modified after Cawood and Buchan 2007; Novo-Fernández et al. 2016). **b** Schematic geological map of the Pannonian Basin (modified after Csontos et al. 1992, 2002). MM, Małopolska Massif

complexes which preserve regional low- to high-grade metamorphism as well as synorogenic sedimentation and magmatism dominated by felsic rocks (Kroner et al. 2008; Kříbek et al. 2009). According to Buda et al. (2000, 2004) and Klötzli et al. (2004), the Carboniferous Mórágy Granite Complex of the Tisza Mega-unit, Carpathian–Pannonian area, Hungary (Figs. 1b and 2), also originated from the southern part of the Moldanubian Zone and could represent a shear-zone-bounded coherent block in allochthonous position.

The Tisza Mega-unit is a large composite structural unit, which is actually an exotic terrane of European Plate origin in the south-eastern part of the basement of the Pannonian Basin (Haas and Péró 2004). It is made up of Variscan crystalline complexes, molasse-type post-Variscan formations and Alpine overstep sequences with variable evolutionary history. Based on the Variscan and early Alpine tectonostratigraphic characteristics, the Tisza Mega-unit was located at the southern margin of the European Plate, east to the Bohemian Massif, prior to a rifting period in the Middle Jurassic (Csontos and Vörös 2004; Haas and Péró 2004; Klötzli et al. 2004; Varga et al. 2007). The existing palaeogeographic reconstructions, however, are quite generic and sometimes contradicting, so further accurate and reliable correlation studies on the Palaeozoic records of the Tisza Mega-unit are needed.

In the Tisza Mega-unit a marine Silurian formation occurs in the subsurface in southern Transdanubia (Oravecz 1964; Kozur 1984; Árkai et al. 1995; Szederkényi 1996). The Szalatnak Slate Formation composed of low-grade organic-rich metapelite, metagreywacke, and metaconglomerate is known from numerous boreholes in the northwestern marginal zone of the Tisza Mega-unit (Fig. 2). Due to petrographic characteristics as well as metamorphic and deformational evolution this metasedimentary sequence has a considerable importance for correlation of the Tisza Mega-unit.

Normally, these very fine-grained rocks consist of high amounts of phyllosilicates, dominantly K-white mica and chlorite, with lesser amounts of quartz and feldspar which are stable in a wide pressure–temperature range (Miyashiro 1994; Frey and Robinson 1999). Using X-ray powder diffraction (XRPD) methods, illite and chlorite 'crystallinity' (IC and ChC, respectively) are expressed by indices and the most common ones are the Kübler index (KI) for IC and Árkai index (ÁI) for the ChC (Kübler 1967; Árkai 1991; Árkai et al. 1995; Kübler and Jaboyedoff 2000). These indices are widely applied for determining the grade of diagenesis and low temperature metamorphism of (meta)pelitic rocks. Additionally, the 'b' cell dimension of K-white mica estimates the pressure conditions (Sassi 1972; Sassi and Scolari 1974; Guidotti and Sassi 1986; Kisch et al. 2006).

A tool to study the thermal alteration of organic-rich metasedimentary rocks is Raman spectroscopy (e.g., Yui et al. 1996; Beyssac et al. 2002; Rahl, et al. 2005; Rantitsch and Judik 2009; Aoya et al. 2010; Wiederkehr et al. 2011; Kouketsu et al. 2014; Lünsdorf et al. 2014; Mori et al. 2016; Lünsdorf et al. 2017). Several authors published empirical geothermometers based on the Raman spectral properties of carbonaceous material (CM), determining peak metamorphic temperatures in the low-grade (Lahfid et al. 2010; Kouketsu et al. 2014) or low- to high-grade (Beyssac et al. 2002; Rahl et al. 2005; Aoya et al. 2010) temperature range.

The major aim of this study is to evaluate the metamorphic conditions and provenance of the Palaeozoic organic-rich metasedimentary Szalatnak Slate Formation from southern Transdanubia, Tisza Mega-unit (Horváthertelend Unit), Hungary (Fig. 2). For this purpose, a multidisciplinary approach including petrography, XRPD, Raman spectroscopy, K–Ar isotopic geochronology and electron microprobe analysis (EMPA) of white mica has been used. Whole-rock geochemistry of the samples has been determined to interpret the provenance area.

Geological setting

The Tisza Mega-unit forms the basement of the Pannonian Basin south of the Mid-Hungarian (Zagreb–Zemplin) Lineament (Fig. 1b) (Csontos and Vörös 2004; Haas and Péró 2004; Schmid et al. 2008). On the north the SW–NE trending Zagorje–Mid-Transdanubian Shear Zone (Pamić and Tomljenović 1998; Haas et al. 2000; Vozár et al. 2010; Fig. 2) comprises a 100 km wide and 400 km long unit between the Periadriatic–Balaton Lineament and the Zagreb–Zemplin Lineament.

The pre-Cenozoic basement of the Hungarian part of the Tisza Mega-unit crops out in the Mecsek and Villány Mts, S Transdanubia. The crystalline complexes and the overlying Palaeozoic and Mesozoic sequences show heterogeneous lithological and metamorphic characteristics (Haas and Péró 2004; Szederkényi et al. 2012). In the studied area, the Palaeozoic formations are predominated by continental sequences. Marine Silurian deposits are present as well. During the Pennsylvanian a molasse-type siliciclastic and locally coal-bearing sequence was deposited, while the Permian is represented by continental red beds with volcanoclastic rocks (Vozár et al. 2010; Szederkényi et al. 2012). The studied Silurian Szalatnak Slate Formation is known in the relatively small and isolated Horváthertelend

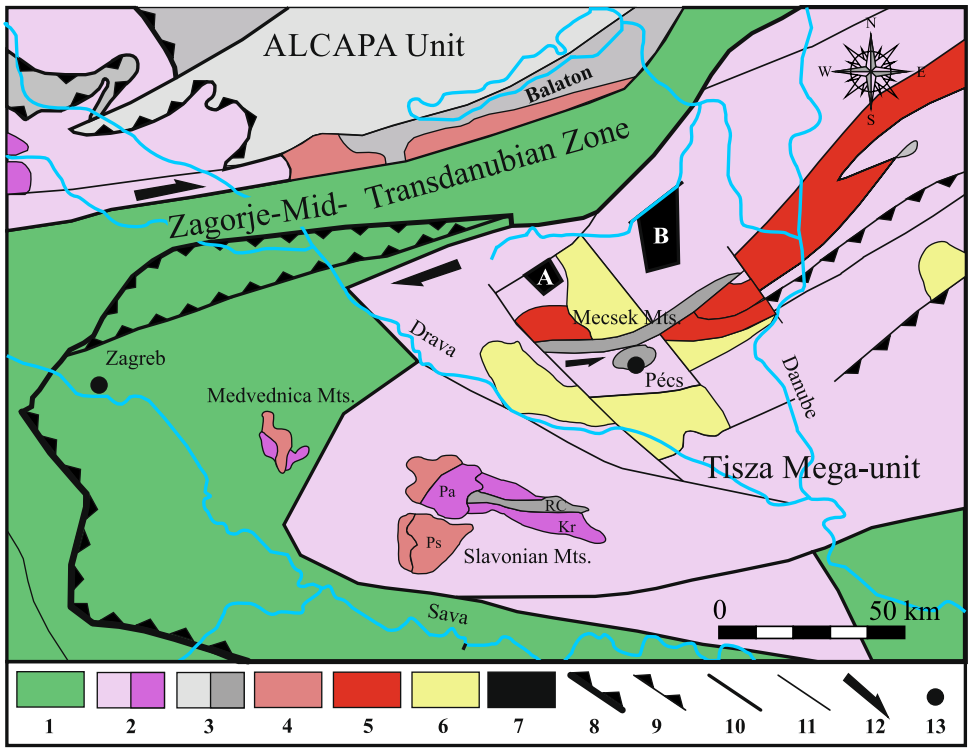

Fig. 2 Tectonostratigraphic map of the Circum-Pannonian region near Transdanubia (Hungary), (modified after Vozár et al. (2010). Symbols: 1, Vardar Zone; 2, Medium to High-grade pre-Alpine metamorphic rocks; 3, Low-grade pre-Alpine metamorphic rocks; 4, Granitoids in general; 5, Late Variscan granitoids; 6, Upper Carboniferous-Permian continental sedimentary rocks; 7, Low-grade Variscan black slate; 8, 1st order thrust fault; 9, 2nd order thrust fault; 10, 1st order normal, reverse and strike-slip fault; 11, 2nd order normal, reverse and strike-slip fault; 12, Displacement direction; 13, Indicated cities; A, Horváthertelend Unit; B, Szalatnak Unit. Kr, Mt. Krndija; Pa, Mt. Papuk; Ps, Mt. Psunj; RC, Radlovac Complex

and Szalatnak Units (Fig. 2). In the surroundings gneiss, and mica schist with amphibolite intercalations as well as Variscan granitoids (durbachites) of the Mórágy Granite Complex form the basement (Szederkényi 1996; Buda et al. 2004). The Szalatnak Slate was penetrated by boreholes (e.g., Horváthertelend-1 and Szalatnak-3; Árkai et al. 1995; Szederkényi 1996) and this is the oldest fossil-bearing formation in the area (Szalatnak Unit; Fig. 3). Despite its regional importance, only sporadic information is available about the metamorphism of the Horváthertelend Unit (Szederkényi et al. 2012). The Szalatnak Slate is composed of black slate, metagreywacke and polymictic metaconglomerate with rare fossiliferous lydite intercalations with a maximum thickness of ~ 500 m (Árkai et al. 1995). According to Oravecz (1964), this formation contains Silurian Hystrichosphaerida (acritarch) remains and graptolite fragments. Muellerisphaeridae microfauna, radiolarians and conodonts were recovered from the siliceous rocks (Kozur 1984; Fülöp 1994), corresponding to the *Pterospathodus amorphognathoides* Zone (Llandovery–Wenlock transition).

Based on the phyllosilicate characteristics and vitrinite reflectance of CM, Árkai et al. (1995) proved an anchi–epizonal metamorphic alteration of the Szalatnak Slate. These authors presumed a contact metamorphic overprint caused by a subvolcanic syenite body, belonging to the Mórágy Granite Complex (Fig. 3). The K–Ar isotopic age of the < 2 µm biotite-rich fraction ranges between *c.* 200 Ma and *c.* 170 Ma. Árkai et al. (1995) presumed a Variscan metamorphic age with a subsequent thermal overprint.

Samples and methods

Detailed macroscopic core investigations from the borehole Horváthertelend–1 (Hh–1) were carried out (Fig. 3). Petrographic studies were conducted on hand specimen ($n = 50$) and thin sections ($n = 75$). A multi-method approach, involving metamorphic petrology, microstructural analysis (Paschier and Trouw 2005), whole-rock and mineral chemistry, Raman CM thermometry, mineralogy using XRPD analysis and K–Ar illite geochronology was applied. Mineral abbreviations follow Whitney and Evans (2010).

Whole rock major and trace element chemistry

A total of six representative slate samples were selected for chemical analysis (Fig. 3). Whole rock major (ICP-ES method) and trace (ICP-MS method) element analyses were performed at the Bureau Veritas Mineral Laboratories (AcmeLabs), Vancouver, Canada. As a quality control, duplicate analyses were performed on selected samples. The accuracy and analytical precision of the analytical methods were also verified against a standard internal (in house) reference material (standard STD SO-19).

In this study, major element ratios are used to characterize the sedimentary protolith of the Horváthertelend metapelite samples, following the chemical classification schemes of Cox et al. (1995), Herron (1988) and Pettijohn et al. (1972). Additionally, selected major (e.g., Ti) and trace (e.g., La, Th, Hf) element parameters and discriminatory diagrams

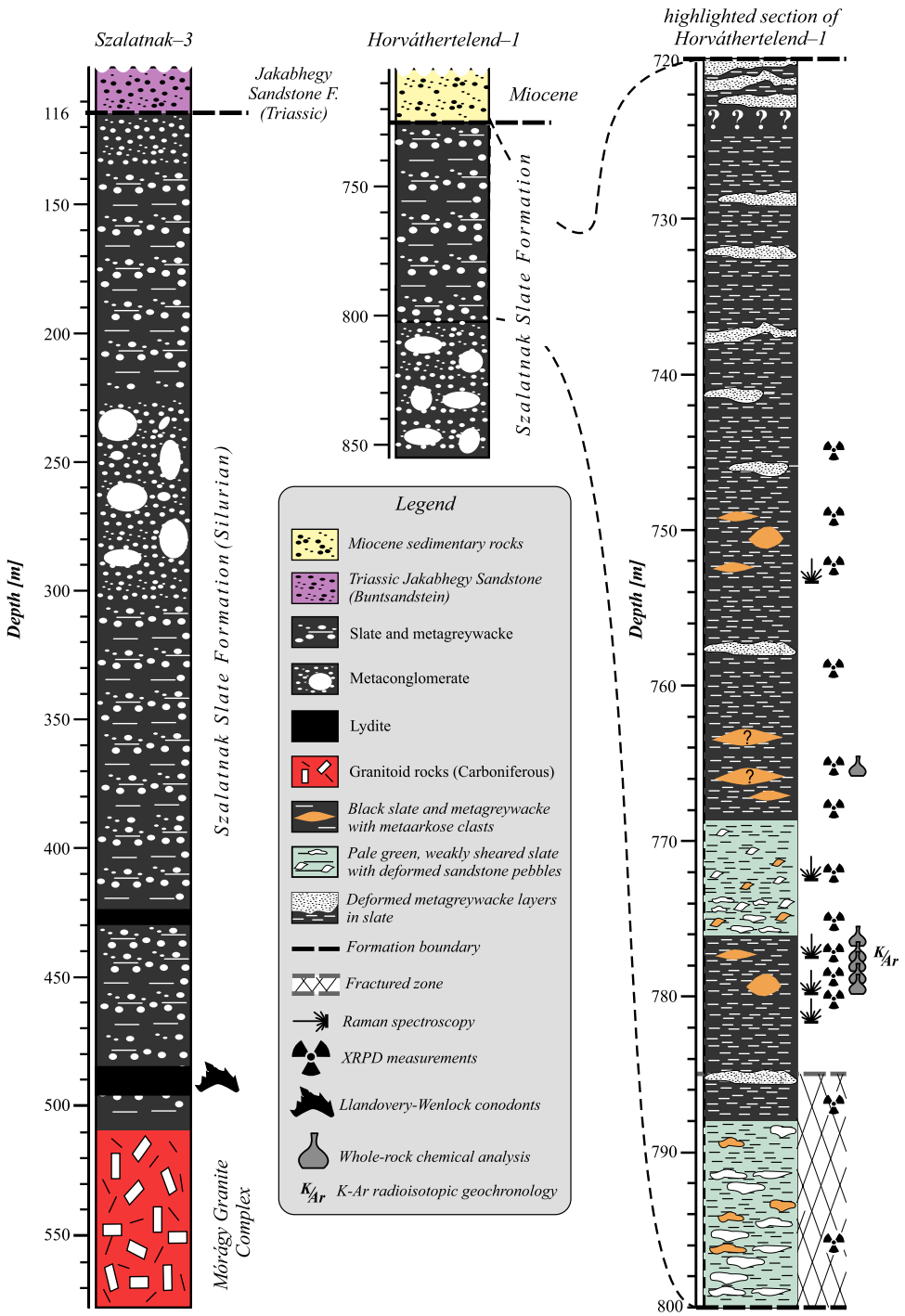

Fig. 3 Schematic lithological columns of the two main sections of the Silurian Szalatnak Slate Formation (modified after Árkai et al. 1996 and Mészáros et al. 2016) showing the positions of the investigated cores within the hole Horváthertelend-1

(Bhatia and Crook 1986; Floyd and Leveridge 1987; Floyd et al. 1989) are used to determine the provenance and tectonic setting.

Raman CM thermometry

Eight samples were selected from the borehole Hh-1 to prepare thin sections normal to the foliation for the Raman analysis. It is well known that CM is sensitive to the polishing process which leads to erroneous Raman spectra (Lünsdorf 2016 and references therein). Lünsdorf (2016) proved that the fine polishing (0.05 µm) influences the Raman spectra of the CM significantly, while all preparation steps before, using coarser slurry, do not. To avoid erroneous measurements, abrasion was carried out in three steps using P800, P1000, and P1200 SiC-abrasive powder. Afterwards the samples were polished in a single step using diamond slurry with a grain size of 6 µm. The Raman spectra of 175 CM

grains were measured using a THERMO Scientific DXR Raman spectrometer. The laser beam was focused beneath the surface of CM grains. The measurements were carried out using an X100 objective lens, a 50 µm pinhole aperture and a 532 nm wavelength Nd-YAG laser with an irradiation power of 2 mW. Every measurement was made using a 900 line/mm grating and the exposure time was 100 s on each individual grain.

The Raman spectrum of CM was fitted by several distinct peaks using peak-fitting software (Peak Fit 4.12 ver.; Sea-Solves Software Inc., MA, USA) with a Voigt function, following the decomposition procedures for Raman CM spectra presented by Kouketsu et al. (2014). For the samples in this study, five distinct bands are identified in the range of 1000–1750 cm^{-1}: ~ 1580 cm^{-1} (G-band), 1350 cm^{-1} (D1-band), 1620 cm^{-1} (D2-band), 1510 cm^{-1} (D3-band) and 1245 cm^{-1} (D4-band). Both calibration procedures of Beyssac et al. (2002) and Kouketsu et al. (2014) were used to provide two independent datasets. Geothermometers proposed by Beyssac et al. (2002), Rahl et al. (2005) and Kouketsu et al. (2014) were applied, respectively.

XRPD and phyllosilicate characterization

The whole rock mineralogical composition and characterization of the separated < 2 µm grain size (clay) fraction were estimated by X-ray powder diffractometry (XRPD). Unaltered, macroscopically homogeneous rock chips were grounded and homogenised in an agate mortar (< 2 min. grinding time per sample). Grain size separation for clay fraction analysis was achieved by repeated ultrasonic deflocculation and gravitational settling. A total of 19 samples were measured by a Rigaku Ultima IV X-ray diffractometer using Bragg–Brentano geometry, CuKα radiation, graphite monochromator, proportional counter, divergence and detector slits of 2/3°.

For whole rock analysis, random powder mounts were made using ~ 0.04 g rock powder on a Si single crystal sample holder to determine the mineralogical composition and to characterize mica polytypes. The specimen were scanned at 50 kV/40 mA from 3 to 70°2θ with a goniometer step rate 1°/min and data acquisition steps of 0.05°. The qualitative evaluation of the XRPD spectra was made by Rigaku PDXL 1.8 software using the ICDD (PDF2010) database. Semi-quantitative mineralogical composition was estimated based on reference intensity ratio (RIR) method.

For clay fraction analysis, highly oriented XRPD slides with 3 mg/cm^2 density were prepared by repeated sedimentation of the separated clay fraction. Both air-dried and ethylene–glycol solvated preparations were scanned at 45 kV/35 mA, from 3 to 50°2θ with goniometer step rate 1°/min and step-width 0.1°. For determination of illite and chlorite 'crystallinity indices' and calculation of crystallite size, a triplicate scan of the same slides were run at 40 kV/30 mA, from 3 to 14°2θ with goniometer step rate 0.6°/min and step-width 0.01°.

The determination of the phyllosilicate 'crystallinity' was made using the Crystallinity Index Standards (CIS) of Warr and Rice (1994) and the Kübler index (KI_{Basel}) calculated after Warr and Mählmann (2015).

For standardization of the Kübler index (KI_{Basel}) and the chlorite 'crystallinity' index (ChC_{CIS}), the Crystallinity Index Standards (CIS) scale was utilized after instructions of Warr and Rice (1994). Instrumental line broadening was determined using an in-house muscovite standard. The narrowest FWHM value measured on the muscovite standard was 0.064° and the sharpest reflection measured for a sample sedimented on a slide was 0.114°. Sample treatment and instrumental conditions for the calibration procedure were strictly the same as during experimental determination of illite and chlorite 'crystallinity indices' of the studied sample set. Analytical quality of the standardization was controlled by 10 subsequent parallel measurements of the same slide. Standard deviation is ~ 2.5% in the case of $FWHM_{10Å} = 0.195$ and $FWHM_{7Å} = 0.198$ ($n = 10$). A good reproduction of the measured values together with a significant correlation were found between $CIS_{Heidelberg}$ (given by the calibration card and Warr and Mählmann 2015) and CIS_{Szeged} using FWHM values of ~ 10 Å reflections ($n = 6$):

$$CIS_{Heidelberg} = 1.096 \times CIS_{Szeged} + 0.144,\ r^2 = 0.960. \quad (1)$$

A less good correlation was arisen for chlorite 'crystallinity' using FWHM values of ~ 7 Å peaks ($n = 4$):

$$CIS_{Heidelberg} = 0.618 \times CIS_{Szeged} + 0.199,\ r^2 = 0.833. \quad (2)$$

The conversation of the CIS scale to KI_{Basel} scale was made according to Warr and Mählmann (2015).

For differentiation between K-, Na- and Ca-rich white micas, the XRPD (00,10) basal reflections around 2 Å were checked using the highly oriented slides (see Frey and Niggli 1972; Árkai et al. 2003, 2004). For a better resolution and precise determination of position of the 00,10 K-white mica peaks, triplicate analyses were made at 50 kV/40 mA, from 40 to 50°2θ with a goniometer scan speed of 0.5°/min and step-width of 0.02°.

K-white mica 'b' cell dimension was measured on random powder mounts made of the separated clay fraction to eliminate the detrital contamination after the proposal of Padan et al. (1982). Triplicate analyses were made at 50 kV/40 mA from 58 to 53°2θ with a goniometer step rate 0.333°/min and data acquisition steps of 0.03°.

Mineral chemistry

K-white mica composition analysis was made with an energy-dispersive and a wavelength-dispersive equipped JEOL JSM-6310 microprobe. The instrument operated at an acceleration voltage of 15 kV, a focal distance of 15 mm and a beam current of ~ 6 nA. Mineral standards were used: adularia (Si, Al, K), garnet (Mg, Fe), rhodonite (Mn), titanite (Ca, Ti), jadeite (Na).

K–Ar dating

K–Ar isotope geochronology was carried out on four slate samples containing a large proportion of K-white mica. For every slate sample, both the whole-rock and the < 2 µm size fraction were measured. These samples do not contain any other K-bearing mineral phase in detectable amount. After crushing in an agate mortar, 1 g of every bulk samples was isolated. The < 2 µm size fraction was separated from aqueous suspension after ultrasonic disaggregation.

Samples were analysed following the procedure of Balogh (1985) at the K–Ar laboratory of the Institute for Nuclear Physics, Hungarian Academy of Sciences, Debrecen. The potassium content was measured on 50 mg sample aliquots after dissolution by HF and HNO_3 using a Sherwood–400 type flame spectrophotometer with an accuracy better than ± 1.5%. Separated mineral sample splits were subjected to heating at 100 °C for 24 h under vacuum to remove atmospheric Ar contamination that adsorbed on the surface of mineral particles during sample preparation. Argon was extracted from the minerals by fusing the samples by high frequency induction heating at 1300 °C. The released gases were cleaned in two steps in a low-blank vacuum system by St-700 and Ti-getters. The isotopic composition of the spiked Ar was measured by a Nier-type mass spectrometer. The atmospheric Ar ratio was analysed each day during the measurement period and averaged 295.9 ± 1.85 (1σ) for 60 independent determinations. This value is not significantly different from the theoretical one (295.5; Nier 1950). All isotope measurements were corrected by the atmospheric $^{40}Ar/^{36}Ar$ ratios determined on the day of the analysis.

The accuracy and reproducibility of the isotope ratio measurements were periodically controlled by the Rodina 2/65 internal standard for which the radiogenic ^{40}Ar content averaged $13.79 \pm 0.12\ (2\sigma) \times 10^{-6}\ cm^3\ g^{-1}$ STP after five independent determinations. The recommended value is $13.71 \times 10^{-6}\ cm^3\ g^{-1}$. The decay constants recommended by Steiger and Jäger (1977) were used for age calculation with an overall error of ± 2%.

Results

Mineralogical composition and rock structure

The studied samples are composed of dark grey—black slate with grey metasiltstone and metasandstone (metagreywacke) intercalations and red metasandstone (metaarkose) clasts up to several cm in diameter (Fig. 4). The lower part of the section (below the depth of 769 m) is, however, predominated by well-foliated pale green—grey slate and monomictic matrix-supported metaconglomerate which contains metasandstone pebbles embedded into a well-foliated fine-grained matrix. The lower part of the metaconglomerate section contains rhyolite pebbles. The samples have a well-developed pressure solution cleavage. The cleavage surfaces are covered by limonitic coatings.

In some samples quartz veins cut through the cores (Figs. 4 and 5). The axial planes of these folded veins coincide with the cleavage planes of the rock. These veins are apparently sheared by pressure solution seams (Fig. 5a). In less-deformed domains of the slate, the original sedimentary lamination is observed. The metasandstone intercalations and clasts are lenticular, often sigmoidal, in shape and occasionally form boudinage structures (Figs. 4 and 5b). Regarding the three principal axes of the clasts, their average axial ratios are *X*/*Z*: ~ 2.8, *Y*/*Z*: ~ 2.7 and *X*/*Y*: ~ 1.0 where X indicates the maximal elongation and Z the maximal shortening direction so the longest axis is parallel to the foliation.

Based on the semi-quantitative XRPD analysis (Supplementary Table 1), the bulk slate samples have a highly variable mineralogical composition with 10—40 mass% K-white mica, 20—50 mass% chlorite, 10—40 mass% quartz and 5—20 mass% albitic plagioclase together with a relatively high amount of amorphous material (up to ~ 5 mass%, dominantly organic matter and limonite). The matrix of the slate has a moderately developed continuous foliation with oriented sericitic K-white mica and chlorite bands. Occasionally, the continuous foliation associates with an anastomosing pressure solution cleavage, having carbonaceous material and limonite (presumably after pyrite) (Fig. 5c). Both in the matrix and in the quartz veins all studied samples contain randomly oriented needle-shaped anatase crystals (~ 50 µm), reflecting prekinematic idio- and hypidioblasts (Fig. 5d). Additionally, both the lenticular metasandstone clasts and the prekinematic anatase grains have chlorite + quartz pressure shadows parallel to the foliation. In the pale-grey slate, these deformation structures have a slightly monoclinic symmetry. The folded pretectonic quartz veins are dynamically recrystallized (Fig. 5d) and the quartz grains have a strongly undulose extinction and subgrain microstructure. Along the serrated grain-boundaries small undeformed neoblasts were formed. In some samples euhedral tourmaline needles

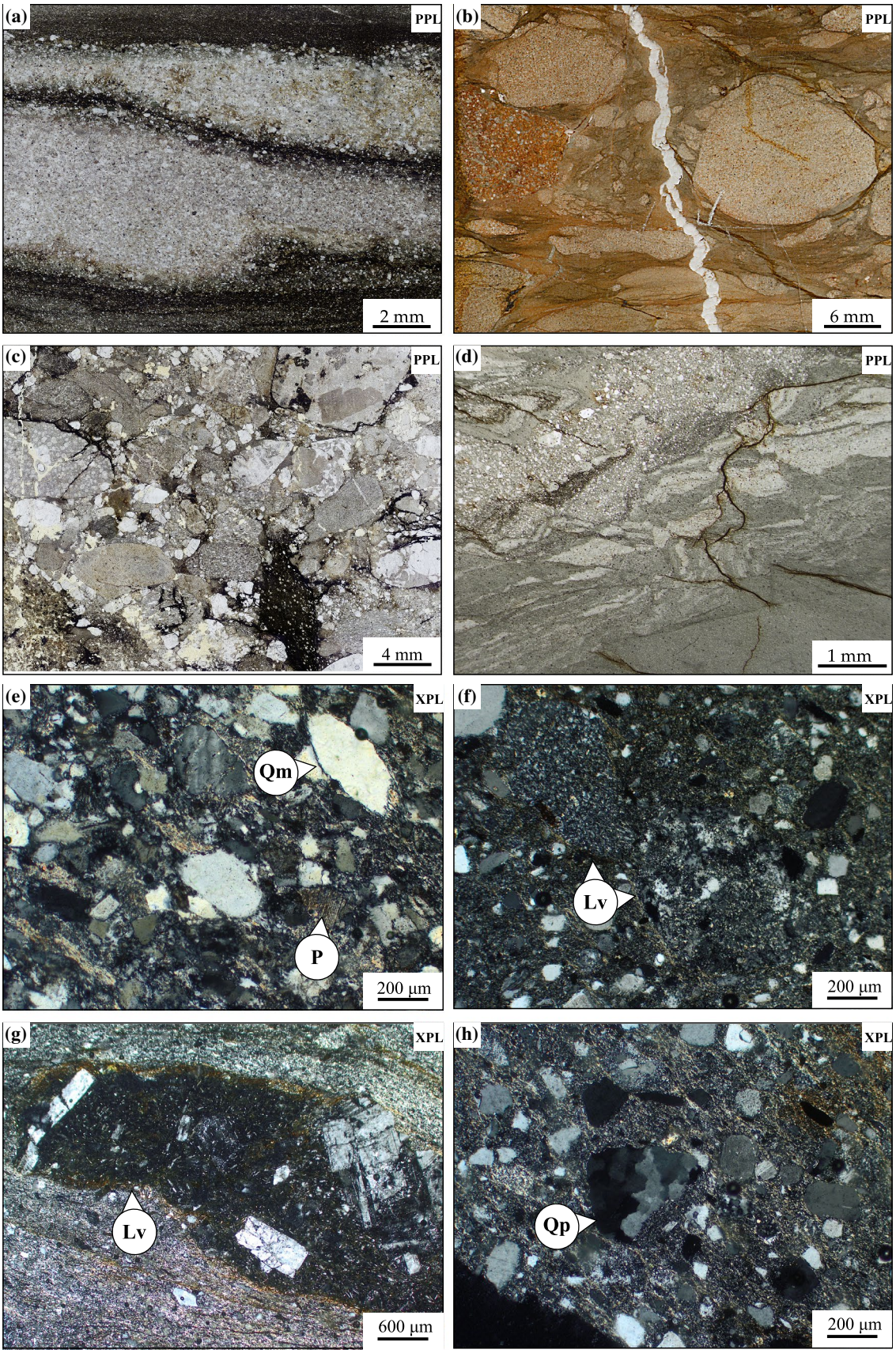
(a)
PPL
2 mm
(b)
PPL
6 mm
(c)
PPL
4 mm
(d)
PPL
1 mm
(e)
XPL
Qm
P
200 μm
(f)
XPL
Lv
200 μm
(g)
XPL
Lv
600 μm
(h)
XPL
Qp
200 μm

◂**Fig. 4** Representative petrographic features of the studied rocks. **a** Metagreywacke intercalations in a foliated metasiltstone sample. **b** Metagreywacke and red metaarkose clasts in a matrix-supported metaconglomerate sample. **c** Grain-supported, polymictic metaconglomerate. **d** Deformed laminae in metagraywacke and slate. Note: the cleavage surfaces are covered by limonitic coatings. **e**–**h** Dominant detrital grain types in the metagreywacke samples. Lv, volcanic lithic fragment; P, detrital plagioclase; Qm, monocrystalline quartz; Qp, polycrystalline quartz; PPL, plane polarized light; XPL, crossed polars

(70−100 µm) are identified in the matrix. They are arranged parallel to the foliation (Fig. 5f).

In the quartz-rich metagreywacke samples matrix materials constitute more than 30% of the rock by volume (up to 40 vol%). Their sand-sized framework grains are composed of quartz (~ 70 vol%), volcanic rock fragments with intermediate composition (~ 20 vol%) and detrital plagioclase (~ 10 vol%) (Fig. 4e–h). The metaarkose clasts are well-sorted, grain-supported quartz-rich metaarkose (Fig. 5g). The clasts have a mineralogical composition of 40−50 mass% quartz, ~ 20 mass% plagioclase, 20−30 mass% K-white mica and ~ 5 mass% chlorite. Feldspars in the metaarkose clasts are highly altered to K-white-mica and quartz pseudomorphs with a hematite impregnation and coating around the grains. Detrital biotite is intensively degraded to chlorite and opaque minerals. Additionally, the relatively large (300 µm−3 mm) pores and small fractures are filled by 7 Å phase (kaolinite; Mészáros et al. 2016) and quartz. In the margins of the clasts, plagioclase disappears while K-white mica and chlorite content increases.

Chemical classification and provenance

The studied Al-rich metapelitic rocks have a high Index of Compositional Variability (ICV; Cox et al. 1995), with $(Fe_2O_3 + K_2O + Na_2O + CaO + MgO + TiO_2)/Al_2O_3$ ratios from 0.67 to 1.03 (Fig. 6a–c; Table 1). High ICV values indicate geochemically immature deposits, suggesting a tectonically active environment (e.g., Cox et al. 1995). Relatively high Fe_2O_3 concentration in a range from 4.2 to 8.4 mass% is likely related to the high chlorite content (Supplementary Table 1).

The TiO_2 versus Ni plot after Floyd et al. (1989) indicates sediments derived from a felsic source area (Fig. 6d). According to the La/Th versus Hf diagram (Floyd and Leveridge 1987) most samples plot in the field of acidic arc (Fig. 6e). Ternary discrimination diagrams for greywackes such as La–Th–Sc and Th–Sc–Zr/10 plots after Bhatia and Crook (1986) confirm that the sedimentary protolith of the Horváthertelend samples was dominantly derived from felsic volcanic rocks, corresponding to the continental island arc field (Fig. 6f). A unique sample in the lower part of the analysed core Section (779.0 m), however, has an active continental margin signature.

The Horváthertelend samples have high total REE contents. The values of ΣREE are between ~ 127 and 260 ppm with significant enrichment downwards in the studied section (Table 1). In a chondrite-normalized (McLennan 1989) REE diagram (Fig. 7), the samples display systematic light REE enrichment trends. Apart from the sample at the maximum depth, the metapelites show quite uniform patterns with a negative Eu anomaly and near-flat heavy REE patterns. These features reflect their derivation from typical fractionated (mature) upper continental crust (Taylor and McLennan 1985; McLennan 1989). On the other hand, the unique sample has the highest ΣREE value and is more enriched in light REEs. These features together with a fractionated heavy REE pattern reflect its higher content in accessories (e.g., zircon).

Geochemical results indicate a dominantly felsic (silicic) source area and point to an intermediate to acidic volcanic arc terrane as an important component of the provenance area. High amounts of metasandstone pebbles in the metaconglomerate, however, indicate that a recycled quartz-rich sediment source is also possible.

Raman spectroscopy

CM flakes are randomly dispersed in the rocks but they are enriched in the pressure solution seams and in some metagreywacke samples. The graphitic material often associates with anatase and altered pyrite, which generally is transformed to goethite. In addition to the autochthonous grain population, a highly ordered, probably allochthonous, graphitic carbon grain population is also present. This highly ordered population has a well-rounded grain-shape and small grain-size (10–15 µm) with a distinctive, ordered Raman spectra, showing strong G band and very weak D1 and D2 bands. This population was excluded from the thermometry procedure because of its assumed detrital origin. The grain population located in microlithons was used in this study for RSCM thermometry due to the lack of shearing deformation.

The autochtonous CM population is a low-grade disordered graphitic material (Table 2). Its spectra display a symmetric D1 band and a negligible D3 band with an average R1 ($D1_{intensity}/G_{intensity}$, Beyssac et al. 2002) ratio of ~ 1.5. D2 defect band forms a distinct shoulder on the G band (Fig. 8). The Raman spectra suggest that the metamorphism took place between ~ 330 and ~ 400 °C maximum metamorphic temperature (Beyssac et al. 2002; Aoya et al. 2010; Lahfid et al. 2010; Kouketsu et al. 2014; Beyssac et al. 2016).

Using the calibration of Beyssac et al. (2002), RSCM thermometry shows a normal distribution with a mode at 351 °C whereas the arithmetic mean of the estimated temperature is 356 ± 21 °C. The modified thermometer of Rahl

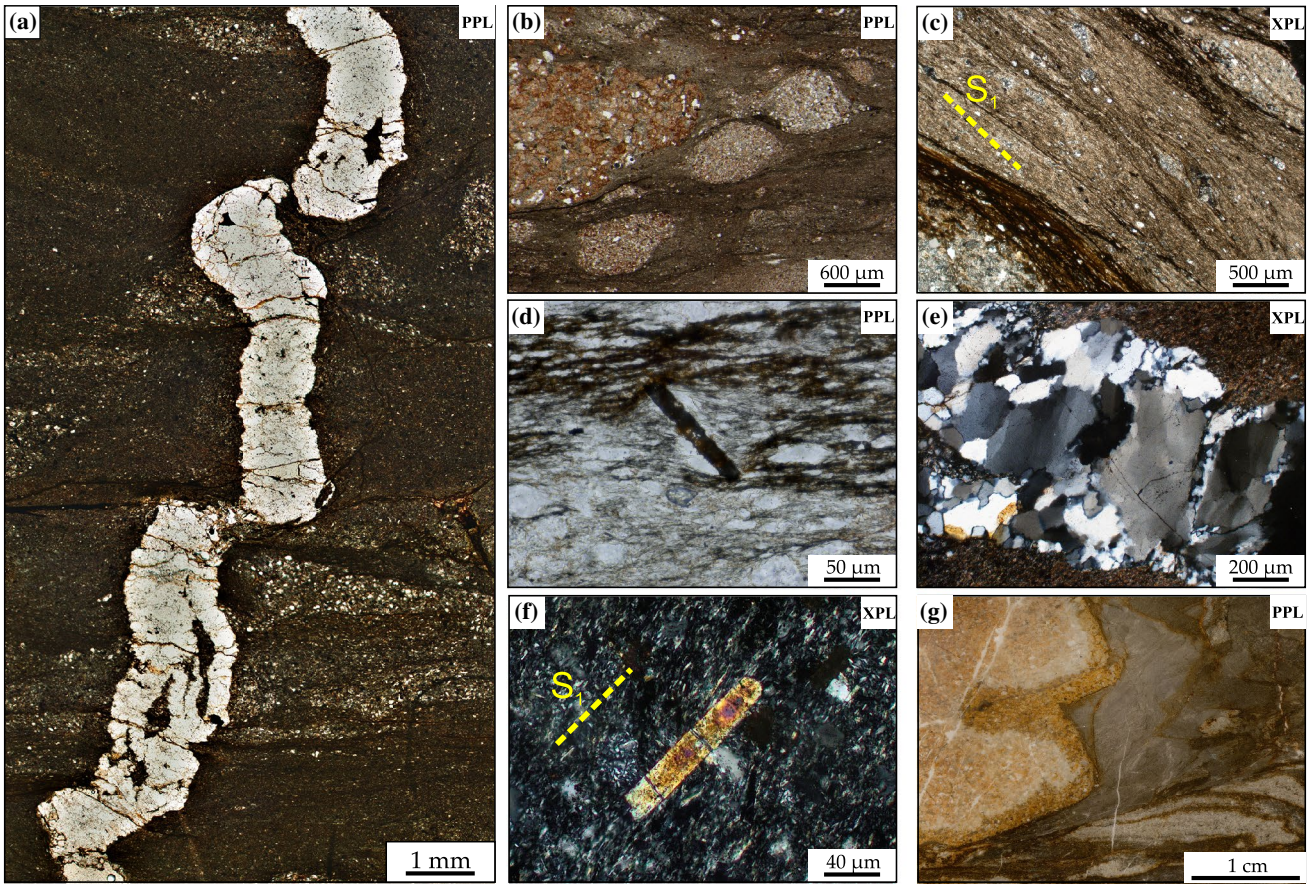

Fig. 5 Characteristic microstructures of the studied slate samples. **a** Pretectonic, recrystallized quartz vein apparently thrusted and folded by pressure solution. **b** Sigmoidal metaarkose and metagreywacke lenses and moderately developed spaced foliation with pressure solution origin. **c** Phyllosilicate-rich band with well-developed continuous foliation and a goethite impregnated pressure solution domain (dark brown band) in slate. Note: S1 secondary foliation has a small angle (5°−10°) to the sedimentary bedding. **d** Weakly asymmetric chlorite + quartz pressure shadow structure around a rigid anatase blast. **e** Recrystallized quartz vein in slate. Unique quartz grains show strong undulatory extinction and subgrain structure. Grains have lobate grain-boundary with small lobes and neoblasts around them indicative of low-temperature grain boundary migration recrystallization (BLG). **f** Epigenic, euhedral tourmaline needle with parallel orientation to the foliation (S1) in slate. **g** Red metaarkose clast in a black, well-foliated slate sample

et al. (2005) shows a mode of 362 °C and a mean temperature of 349 ± 35 °C. Obviously, the mode provides a better estimation of the expected value of the metamorphic temperature than does the arithmetic mean because of the skewness of the distribution. The applied thermometers suggest an estimated peak metamorphic temperature of ~ 350−370 °C.

X-ray powder diffraction examination of the < 2 µm fraction

The mineralogical composition of the < 2 µm fraction is K-white mica + chlorite + quartz ± albite ± kaolinite (Supplementary Table 1). Kaolinite-bearing samples were excluded from the chlorite 'crystallinity' determinations because of the resulted interference of 001 peak of the kaolinite and 002 peak of the chlorite at ~ 7 Å.

Characteristic *d* spacings of the K-white mica (3.74 Å, 3.00 Å, 2.80 Å) indicate a predominance of the $2M_1$ polytype. The position of the 00,10 reflection estimates a 1.995–2.001 Å *d* spacing. There is no shoulder observable on any sides of this peak, suggesting a near-theoretical 'muscovite' composition for the K-white mica without any Na- or Ca-substitutions referring 'mixed' K-Na-mica (Livi et al. 1997). According to the ethylene glycol treatment of the samples, neither K-white mica nor chlorite contains any interstratified smectitic swelling phase.

Esquevin index of the K-white mica, i.e., intensity ratio of the 5 Å and 10 Å peaks (Esquevin 1969), shows a phengitic composition for most of the studied samples (Fig. 9a, Table 3). After Dunoyer de Segonzac (1970) and Árkai et al. (1995), only samples with > 0.25 Esquevin index were used to determine the KI (Kübler 1964; Kübler and Jaboyedoff 2000). The KI_{Basel} values cover a range from 0.19 to 0.38

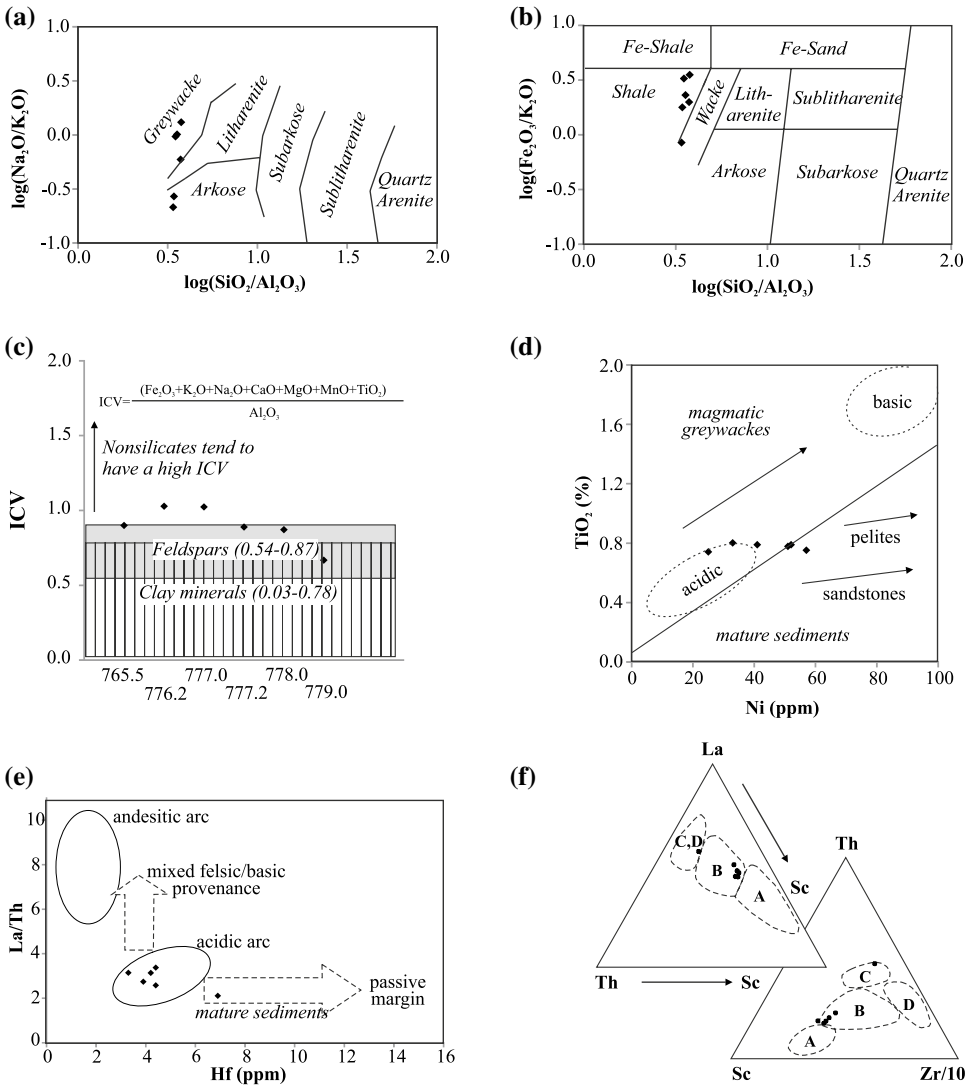

Fig. 6 Chemical classification and provenance diagrams of the selected Horváthertelend samples. **a** Chemical classification scheme of siliciclastic sediments based on major elements (Pettijohn et al. 1972). **b** Chemical classification scheme of Herron (1988). **c** Values for the Index of Compositional Variability (ICV; Cox et al. 1995) for the studied Horváthertelend slate samples. **d** Characterization of the source rock composition based on TiO_2–Ni diagram after Floyd et al. (1989). **e** La/Th versus Hf provenance discrimination diagram (Floyd and Leveridge 1987). **f** Ternary discrimination diagrams for greywackes after Bhatia and Crook (1986). Abbreviations for tectonic settings are as follows: A, oceanic island arc; B, continental island arc; C, active continental margin; D, passive margin

$\Delta°2\theta$ with a mean of 0.22 ± 0.04 $\Delta°2\theta$ (Fig. 9b; Table 3). The ChC_{CIS} values range from 0.27 to 0.53 $\Delta°2\theta$ with a mean of 0.31 ± 0.06 $\Delta°2\theta$ (Fig. 9c, Table 3). Between the KI_{Basel} and ChC_{CIS} values a moderate correlation ($R = 0.77$) is observed (Fig. 10). The mean crystallite size of the K-white mica calculated applying the Scherrer-equation (Klug and Alexander 1974; Merriman et al. 1990) falls between 288 ± 14 Å and 1293 ± 54 Å. Estimated mean crystallite size based on the chlorite 002 reflection fluctuates from 157 ± 4 Å to 1043 ± 43 Å. The calculated mean crystallite size values, excluding the anomalous values of the altered samples (745.1b, 779.6 and 787), are 890 ± 198 Å for K-white mica and 692 ± 175 Å for chlorite (Table 3).

Because of the K-white mica + chlorite + quartz + albite ± anatase mineral assemblage and the absence of paragonite, pyrophyllite or chloritoid indicative for Al-saturated metapelites (Franceschelli et al. 1989), the method and the scale of Guidotti and Sassi (1986) are applied. Due to the high amount of CM reducing (low f_{O2}) conditions are presumed during metamorphism, and primary origin of hematite or goethite are ruled out. The measured 'b' cell dimension values range from 9.011 to 9.029Å with a mean of 9.019 ± 0.004 Å (Fig. 9d).

Mineral chemistry

The Si content of the K-white mica ranges between 6.26 and 6.73 apfu. Fe^{2+} content varies between 0.28 and 0.38 and the Mg ranges between 0.34 and 0.57. The calculated Na/(Na + K) ratios fluctuate between 0.02 and 0.08 (Supplementary Table 2).

Geochronology

The K–Ar radioisotopic age data of the whole rock samples and those of the < 2 µm grain-size fraction fall in the range

Table 1 Whole rock major and trace element composition of the studied slate samples

	Samples					
	765.5	776.2	777	777.2	778	779
Major elements (in mass%)						
SiO_2	61.59	62.48	60.14	62.87	63.61	64.18
Al_2O_3	17.93	16.60	17.17	17.59	17.01	18.87
Fe_2O_3	7.00	7.72	7.99	6.19	6.02	4.00
MgO	2.81	3.19	3.68	2.92	2.92	2.05
CaO	0.46	0.28	0.26	0.30	0.29	0.08
Na_2O	1.06	2.86	2.36	2.71	1.79	1.01
K_2O	3.95	2.19	2.45	2.69	3.03	4.73
TiO_2	0.77	0.76	0.74	0.76	0.72	0.71
P_2O_5	0.30	0.12	0.11	0.13	0.16	0.05
MnO	0.09	0.07	0.10	0.08	0.05	0.03
LOI	3.80	3.50	4.80	3.60	4.20	4.10
Total	95.96	96.27	95.00	96.24	95.60	95.71
ICV	0.90	1.03	1.02	0.89	0.87	0.67
Trace elements (in ppm)						
Ba	543	418	430	469	488	681
Ni	33	52	51	41	57	25
Sc	21	21	20	21	20	17
Be	4.0	6.0	< 1	1.0	2.0	3.0
Cr	13	15	14	15	16	18
Co	18.2	23.5	22.8	20.2	23.0	8.4
Cs	4.3	2.8	4.6	3.9	3.5	6.5
Ga	26.6	18.5	23.4	21.5	17.8	21.6
Hf	4.4	4.2	3.3	3.9	4.4	6.9
Nb	10.3	8.1	8.7	10.5	8.0	12.4
Rb	120.9	71.2	75.7	84.4	94.1	155.6
Sn	3.0	1.0	3.0	2.0	2.0	3.0
Sr	64	156	121	148	94	89
Ta	0.7	0.6	0.6	0.7	0.9	0.8
Th	9.6	8.1	8.1	8.7	8.7	29.0
U	2.2	2.9	2.4	2.4	2.4	7.5
V	128	141	125	134	124	122
W	2.9	3.0	2.2	2.7	2.2	4.3
Zr	144	146	122	139	149	240
Y	28.9	20.5	20.8	24.2	20.7	23.7
La	24.8	25.4	25.5	23.9	29.4	61.3
Ce	57.4	53.5	53.7	53.9	60.7	117.2
Pr	6.9	6.1	6.4	6.0	7.0	12.2
Nd	26.1	23.1	23.6	22.3	27.7	43.4
Sm	5.47	4.17	4.90	4.58	4.91	6.68
Eu	1.14	0.93	1.09	0.99	1.13	1.71
Gd	4.77	3.96	4.53	4.46	4.31	6.03
Tb	0.75	0.59	0.69	0.68	0.65	0.84
Dy	5.21	3.85	4.18	4.36	4.05	4.80
Ho	1.12	0.77	0.79	0.93	0.77	0.82
Er	3.02	2.25	2.54	2.84	2.57	2.46
Tm	0.51	0.36	0.36	0.39	0.37	0.36
Yb	3.03	2.47	2.40	2.69	2.57	2.21
Lu	0.46	0.39	0.41	0.43	0.41	0.34

Table 1 (continued)

	Samples					
	765.5	776.2	777	777.2	778	779
ΣREE	141	128	131	128	147	260

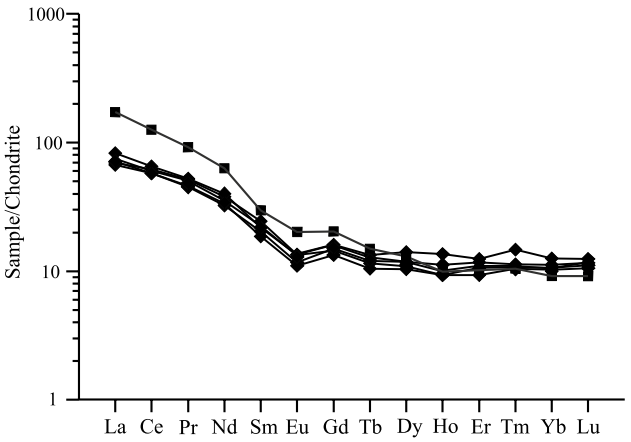

Fig. 7 Chondrite-normalized (McLennan 1989) rare earth element (REE) patterns of the Horváthertelend slate samples. Apart from a unique sample collected from the maximum depth of the core (square), the metapelites show quite uniform patterns (diamond), reflecting their derivation from typical fractionated (mature) upper continental crust

of 302–319 Ma and 288–300 Ma, respectively (Table 4). The K–Ar isochron method (Shafiqullah and Damon 1974) is used to demonstrate extraneous argon or argon loss in a co-genetic suite of samples of different K-contents or the presence of detrital minerals. Two arrays of data can be distinguished on the diagram and the fitted lines intersect the $^{40}Ar/^{36}Ar$ axis close to the atmospheric value at 295.5. This indicates that the two sample sets are co-genetic and post-genetic thermal processes did not result in argon loss or gain from the samples. Whole rock data yield an isochron age of *c.* 312 Ma and the separated < 2 μm fraction samples yield an age of *c.* 297 Ma (Fig. 11).

Discussion

Metamorphic conditions and age

Thermometers of Beyssac et al. (2002) and Kouketsu et al. (2014) give temperature estimations in the range of errors of RSCM methods. For the Szalatnak Slate, the peak temperature of metamorphism is estimated ~ 350–370 °C and shows homogeneous distribution along the studied Horváthertelend section. The XRPD-based phyllosilicate 'crystallinity' data suggest a metamorphic grade corresponding to the ~ 350 °C temperature.

In most of the samples, KI values indicate a K-white mica formation during epizonal metamorphic conditions (Kübler and Jaboyedoff 2000; Warr and Rice 1994) and suggest a low-grade metamorphism. Based on the I 5 Å/I 10 Å ratios (Esquevin 1969) and EMPA data, these K-white mica populations are phengitic in composition which is common in low-grade epizonal conditions (Erns 1963; Frey and Robinson 1999; Massonne and Schreyer 1987; Velde 1965). The CIS calibrated Árkai indices, however, indicate anchizonal metamorphic conditions (zone boundaries after Kübler and Jaboyedoff 2000 correlated with ChC_{002} in Árkai 1991). Nevertheless, the correlation between the KI_{Basel} and ChC_{CIS} values indicates a genetic relationship between the phengitic K-white mica and chlorite in the studied rocks. The

Table 2 Estimated metamorphic temperatures of the studied samples based on Raman spectroscopy of the carbonaceous material

Depth (m)	*n*	R1	R2	*T* (°C)[a]	*T* (°C)[b]	FWHM D1 (cm^{-1})	FWHM D2 (cm^{-1})	*T* (°C)[c]	*T* (°C)[d]
753.0	28	1.42 ± 0.25	0.63 ± 0.06	360 ± 26	352 ± 43	52.3 ± 10.9	24.7 ± 3.5	364 ± 24	367 ± 28
772.3	23	1.65 ± 0.25	0.64 ± 0.06	358 ± 25	356 ± 30	51.9 ± 6.6	26.4 ± 3.6	366 ± 14	356 ± 24
777.0	22	1.40 ± 0.26	0.64 ± 0.04	356 ± 20	340 ± 26	57.6 ± 12.5	27.7 ± 3.2	354 ± 27	347 ± 22
779.6	19	1.47 ± 0.21	0.64 ± 0.05	356 ± 23	348 ± 42	59.9 ± 14.2	28.1 ± 3.3	349 ± 31	344 ± 23
780.3	20	1.42 ± 0.17	0.63 ± 0.04	360 ± 19	354 ± 34	56.8 ± 13.3	27.3 ± 2.6	356 ± 29	350 ± 18
780.0	18	1.50 ± 0.15	0.64 ± 0.05	353 ± 22	344 ± 44	59.5 ± 12.7	27.0 ± 6.1	350 ± 28	352 ± 41
781.0	25	1.64 ± 0.15	0.63 ± 0.02	357 ± 9	363 ± 17	53.5 ± 8.7	26.0 ± 3.5	363 ± 19	359 ± 24
790.0	15	1.45 ± 0.20	0.63 ± 0.04	357 ± 20	349 ± 32	61.2 ± 10.1	26.3 ± 2.4	346 ± 22	357 ± 17
Sum	170	1.50 ± 0.26	0.27 ± 0.04	356 ± 21	349 ± 35	56.1 ± 11.5	26.6 ± 3.7	365 ± 25	355 ± 25

FWHM, full width at half maximum

Temperature estimation using thermometer of [a]Beyssac et al. (2002); [b]Rahl et al. (2005); Kouketsu et al. (2014) based on [c]D1 band and [d]D2 band

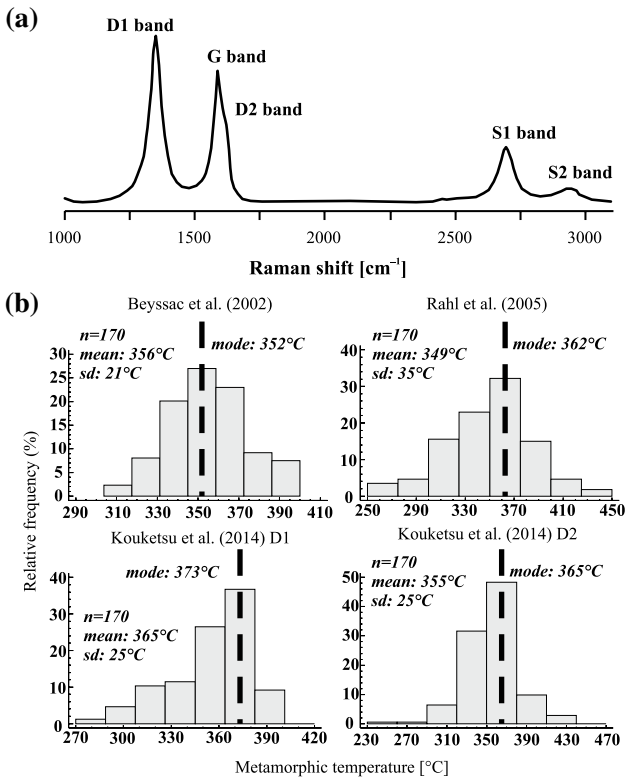

Fig. 8 **a** Raman spectra of the graphitic carbonaceous material (CM) in the studied samples. **b** Summarized histograms and statistical parameters of each RSCM thermometer characteristic for the whole studied slate unit

calculated crystallite sizes of the white mica and the chlorite are also consistent with this observation.

The 'b' cell dimension values of 9.00 Å–9.04 Å of the K-white mica in the < 2 μm grain size fraction are characteristic of a medium pressure geodynamic environment (Fig. 12) during the formation of K-white mica in the ms + chl + qz + ab ± ant assemblage (Guidotti and Sassi 1986; Sassi F 1972; Sassi and Scolari 1974). The estimated 2.5−4 kbar pressure supports this conclusion.

The characteristic deformational microstructures, such as the pervasive continuous foliation, the moderately developed pressure solution cleavage and chl + ms + qz mica beards in pressure shadows, indicate diffusional mass transfer. Deformed vein quartz with subgrain structure and neoblasts along its margins are indicative of a low-temperature grain boundary migration recrystallization (Paschier and Trouw 2005; Stipp and Kunze 2008; Stipp et al. 2002). These features correspond to epizonal thermal conditions during the deformation as well (Paschier and Trouw 2005; Stipp et al. 2002). The appearance of the deformational microstructures indicates flattening strain based on the principal axis of the clasts (Flinn 1962; Ramsey and Huber 1983).

The whole rock and the separated < 2 μm fraction mean ages slightly differ (310.1 ± 8.1 Ma and 293.1 ± 7.7 Ma, respectively). The K–Ar age increases with the increasing grain-size which is considered as detrital effect or multiphase K-white mica crystallization (Clauer and Chaudhuri 1995; Clauer and Weh 2014). Based on the petrographic and XRPD examinations, only the K-white mica is a stoichiometrically K-bearing mineral phase. The K-white mica is regarded as product of a single, progressive metamorphic event. Therefore, both studied grain-size fractions suffered resetting near the closure temperature of phengitic K-white mica (~ 350 °C in the case of coarse-grained crystals; Hunziker 1986; Hunziker et al. 1986). Consequently the K–Ar radioisotopic age of < 2 μm size fraction with lower closure temperature (~ 260 °C; Hunziker 1986; Hunziker et al. 1986) is considered as a cooling age (Glasmacher et al. 2001). The relatively small K–Ar age difference of the grain-size fractions supports the cooling age model rather than the detrital effect. Because the estimated peak metamorphic temperature is higher than the closure temperature a resetting of the K–Ar isotopic system is assumed (Leitch and McDougall 1979). The K–Ar data of the < 2 μm suggest post-Variscan (*c.* 290 Ma) uplift while the whole rock age data show a Variscan (*c.* > 310 Ma) metamorphism.

Regional correlation

The Tisza Mega-unit is a large lithosphere block of complex internal structure. From the point of view of the palaeogeographic reconstruction, this exotic terrane was often neglected, or its role in the regional correlation was not carefully considered (Haas and Péró 2004). Verniers et al. (2008) provided an extensive review of the available literature for outcrop areas and subsurface presence of the Silurian in Central Europe, including some Slavonian occurrences in the Tisza Mega-unit (Mt. Psunj, Mt. Papuk and Mt. Krndija; Fig. 2). Unfortunately, however, there was no mention about Hungarian records in that article.

The most intensively studied metasediments of the Tisza Mega-unit are located in the Slavonian Mts. (Croatia) (e.g., Balen et al. 2015; 2018). The Radlovac Complex (Fig. 2) consists of slates, phyllites, metagreywackes and metaconglomerates with local (meta)basic intrusions (Pamić and Jamičić 1986; Jamičić 1988). In spite of some lithological similarity, however, the Radlovac metasedimentary rocks significantly differ from those of the Horváthertelend Unit. The possible presence of Late Silurian slates, belonging to the Noric–Bosnian Terrane of peri-Gondwana (Verniers et al. 2008), was mentioned by Jerenić et al. (1994). Nevertheless, in the Radlovac Complex Pennsylvanian and Permo triassic rocks are dominantly exposed with Alpine low-T regional metamorphism (Bišević et al. 2010, 2011, 2013).

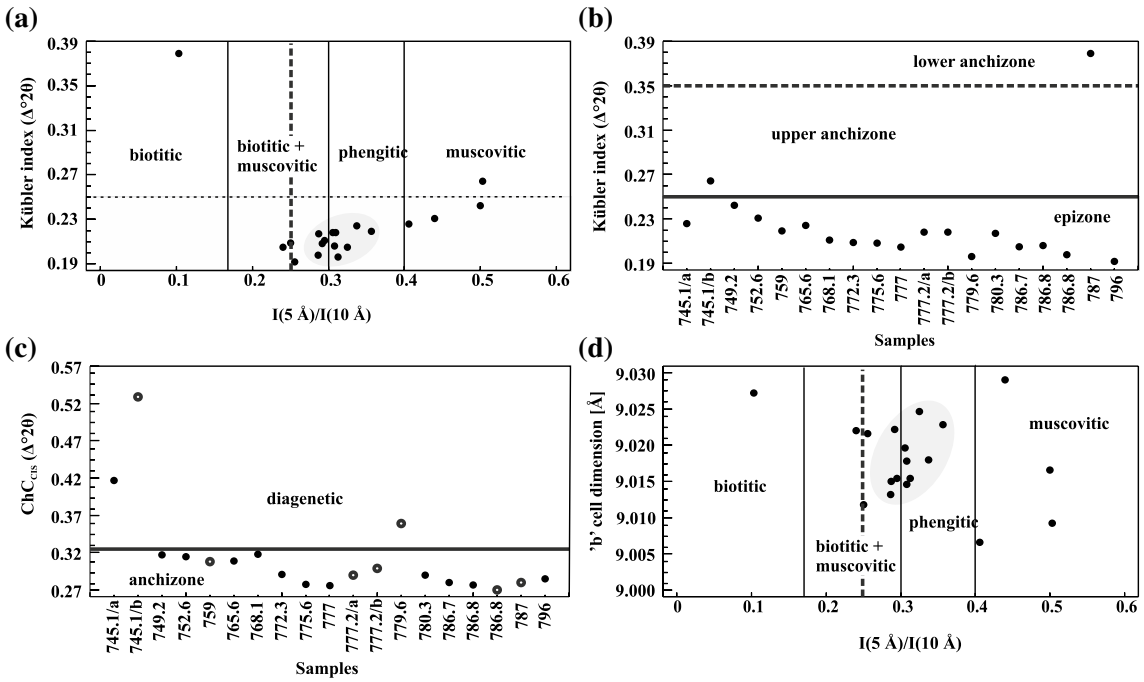

Fig. 9 **a** Esquevin index versus KI_{Basel} values plot (after Esquevin 1969) suggests dominantly phengitic K-white mica composition of most samples. **b** KI_{Basel} plot indicates epizonal metamorphism of the formation. Zone boundaries are indicated after Kübler and Jaboyedoff (2000) and Warr and Mählmann (2015). **c** ChC_{CIS} plot shows chlorite 'crystallinity' values of the studied samples. Note: empty circle indicates the presence of kaolinite in the studied sample. **d** Esquevin index versus 'b' cell dimension diagram of the samples. The highlighted area indicates samples suitable for pressure characterization

Table 3 XRPD parameters of the 10 Å and 14 Å mineral phases of the < 2 µm fraction

Sample (m)	I(5 Å)/I(10 Å)	d_{0010} (Å)	KI_{Basel} (Δ°2θ)	ChC_{CIS} (Δ°2θ)	K-white mica crystallite size (Å)	$Chlorite_{002}$ crystallite size (Å)	'b' cell dimension (Å)
745.1a	0.41	2.000	0.226 ± 0.003	0.417 ± 0.045	739 ± 24	250 ± 48	9.007 ± 0.006
745.1b	0.50	2.001	0.264 ± 0.015	0.529 ± 0.009	528 ± 61	157 ± 4	9.009 ± 0.007
749.2	0.50	2.000	0.242 ± 0.005	0.317 ± 0.003	625 ± 30	483 ± 14	9.017 ± 0.005
752.6	0.44	1.999	0.231 ± 0.000	0.315 ± 0.001	701 ± 3	497 ± 4	9.029 ± 0.005
759	0.36	1.998	0.219 ± 0.002	0.308 ± 0.001	804 ± 18	537 ± 10	9.023 ± 0.002
765.6	0.31	1.999	0.224 ± 0.001	0.309 ± 0.004	757 ± 10	531 ± 24	9.018 ± 0.003
768.1	0.30	1.998	0.211 ± 0.004	0.318 ± 0.002	894 ± 45	478 ± 10	9.015 ± 0.003
772.3	0.25	1.997	0.209 ± 0.005	0.291 ± 0.002	926 ± 65	669 ± 16	9.012 ± 0.006
775.6	0.29	1.997	0.208 ± 0.001	0.278 ± 0.000	941 ± 13	853 ± 6	9.022 ± 0.003
777	0.24	1.997	0.205 ± 0.002	0.276 ± 0.002	1061 ± 75	897 ± 52	9.022 ± 0.002
777.2a	0.31	1.997	0.218 ± 0.001	0.290 ± 0.001	813 ± 14	682 ± 9	9.020 ± 0.003
777.2b	0.31	1.997	0.218 ± 0.003	0.299 ± 0.001	817 ± 28	598 ± 7	9.015 ± 0.005
779.6	0.31	1.998	0.196 ± 0.001	0.359 ± 0.010	1193 ± 37	341 ± 23	9.015 ± 0.002
780.3	0.27	1.999	0.217 ± 0.001	0.290 ± 0.002	825 ± 11	683 ± 15	9.015 ± 0.003
780.4	0.32	1.997	0.205 ± 0.002	0.280 ± 0.002	992 ± 41	809 ± 30	9.025 ± 0.002
786.7	0.31	1.997	0.206 ± 0.003	0.277 ± 0.003	979 ± 55	876 ± 48	9.018 ± 0.000
786.8	0.29	1.997	0.198 ± 0.001	0.270 ± 0.003	1144 ± 36	1043 ± 82	9.013 ± 0.005
787	0.10	1.995	0.379 ± 0.014	0.280 ± 0.001	288 ± 14	813 ± 18	9.027 ± 0.005
796	0.26	1.996	0.192 ± 0.001	0.285 ± 0.003	1293 ± 54	745 ± 38	9.022 ± 0.003

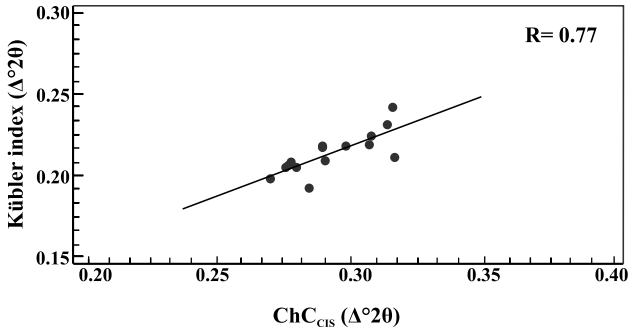

Fig. 10 Kübler index versus chlorite 'crystallinity' index (ChC_{CIS}) plot of the studied samples from the borehole Horváthertelend-1

In the surrounding area of the Tisza Mega-unit, the graptolite-bearing Silurian deposits in the Medvednica Mountain (Croatia; Fig. 2) belong to the distal sedimentary successions on peri-Gondwana, Eastern Alps (Verniers et al. 2008) which passed through Alpine prograde metamorphism as well (Judik et al. 2008; Rantitsch and Judik 2009). Further west, the Silurian of the Carnic Alps (Fig. 13), corresponding to the Proto-Alps Terrane, displays a northern Gondwana appearance. Sequences consist typically of either black shales or calcareous shales and limestones with a low terrigenous influx (Verniers et al. 2008). Consequently, the abovementioned Silurian rocks have no direct importance for palaeogeographic correlation of the study area with a conglomerate-bearing proximal succession.

Previous works on correlation of the Tisza Mega-unit (Buda et al. 2000) pointed out that there are similarities in lithology and in Variscan evolutionary history of the southern Transdanubian area and the Moldanubian Zone of the Bohemian Massif. The Variscan Mórágy Granite known from the SW Tisza Mega-unit was correlated with the Variscan durbachitic granitoid plutons of the central and eastern Bohemian Massif (Gy et al. 2004; Klötzli et al. 2004; Varga et al. 2003) highlighted petrographic and geochemical similarities between the Pennsylvanian continental Téseny Sandstone, Transdanubia (Hungary), and the Cracow Sandstone, Upper Silesian Coal Basin (Poland). Furthermore, the protolith and metamorphic evolution of the sporadic serpentinite occurrences of the SW Tisza Mega-unit (Gyód and Helesfa Serpentinite) reflect a close relationship with the serpentinite bodies of the Góry Sowie Massif in the W Sudetes (Kovács et al. 2009, 2016).

In the Bohemian Massif, numerous occurrences of Silurian sedimentary sequences are known (Fig. 13). The most characteristic territories are the Barrandian Basin (Prague Basin, corresponding to the Silurian Perunica Terrane), the'Islet Zone', the Železné Hory Mts and the Hlinsko and the Lužice Regions (Suchý et al. 2002, 2015; Štorch 1999; Štroch and Kraft 2009). The Silurian succession of the Prague Basin was only slightly deformed (Verniers et al. 2008). In contrast, the Silurian successions of the 'Islet Zone' passed through contact and regional metamorphism. In the Moravo-Silesian Zone of the Brunovistulicum, only a unique Silurian occurrence is known in the Drahany Highland near the village of Stínava (Kalvoda et al. 2008, Verniers et al. 2008).

It is important to note, however, that the Silurian sediments of the Bohemian Massif belong to the distal

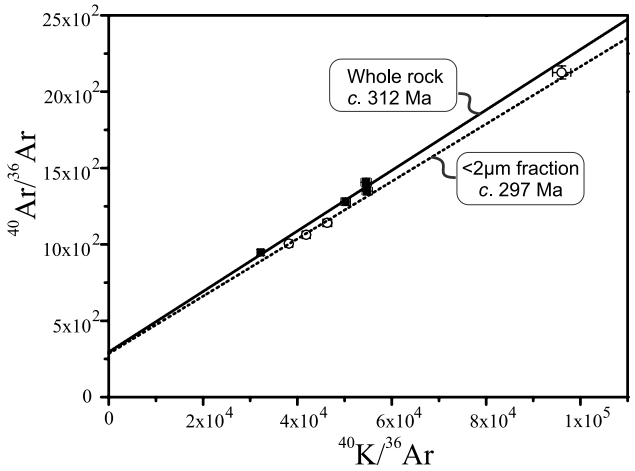

Fig. 11 $^{40}K/^{36}Ar$ versus $^{40}Ar/^{36}Ar$ isochron plot of the analysed whole rock (solid line) and separated < 2 μm grain-size fractions (dashed line)

Table 4 Results of the K–Ar analysis of the whole rock and the < 2 μm grain-size fraction

Sample	Depth (m)	Size fraction	*K* (%)	$^{40}Ar_{rad}$ (10^{-6} cm^3/g)	$^{40}Ar_{rad}$ (%)	Age (Ma + *1*σ)
1-01-B	777.2–778.0	Whole rock	1.98	26.14	68.8	311.8 ± 7.9
1-01-2 M	777.2–778.0	< 2 μm	3.04	37.70	70.6	293.5 ± 7.9
1-02-B	777.2–778.0	Whole rock	2.19	29.77	79.0	319.4 ± 8.2
1-02-2 M	777.2–778.0	< 2 μm	3.29	40.20	72.2	289.8 ± 7.7
1-03-B	777.2–778.0	Whole rock	2.55	33.32	76.9	308.0 ± 8.0
1-03-2 M	777.2–778.0	< 2 μm	3.63	44.13	74.1	288.5 ± 7.6
1-04-B	777.0	Whole rock	3.16	40.52	78.1	302.8 ± 7.8
1-04-2 M	777.0	< 2 μm	4.32	54.92	86.1	300.5 ± 7.6

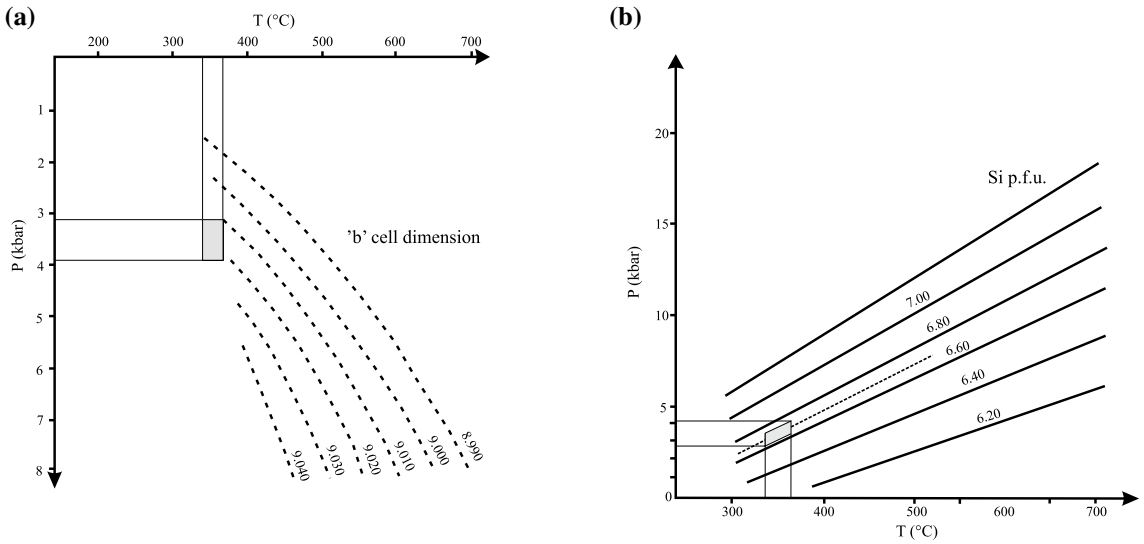

Fig. 12 **a** *P–T* plot with 'b' cell dimension isopleths (modified after Guidotti and Sassi 1986). The grey rectangle indicates the estimated *P–T* interval for the studied samples using the estimated RSCM T_{max} and 'b' cell dimension data. **b** *P–T* plot with K-white mica Si content isolines (modified after Massonne and Szpurka 1997)

sedimentary successions on northern Gondwana and peri-Gondwana (Verniers et al. 2008 and references therein). The Silurian sequences are black shales or calcareous shales and basinal limestones (Fig. 13). Additionally, the sedimentation was influenced by volcanic activity with deposition of lava flows, tuffs, volcaniclastics as well as tuffaceous limestones (Verniers et al. 2008).

Eastwards from the Bohemian Massif, in the foreland of the Variscan orogen, widespread occurrences of more proximal non-metamorphosed Silurian sequences are known (Łysogóry Region and Małopolska Massif, Holy Cross Mountains, Poland), belonging to the Baltica Terrane (Verniers et al. 2008). In the northern Łysogóry Region (N Holy Cross Mts), the Silurian begins with black graptolite shale (Llandovery–Wenlock) which turns into sandy shale, siltstone and greywacke in the Ludlow–Pridoli. In this sequence carbonate rocks are known in subordinate amounts forming interbeds and lenses (Kozłowski 2008).

To the south from the Łysogóry Region, in the Kielce Region (N Małopolska Massif, S Holy Cross Mts) the Silurian shows similarities to the Łysogóry occurrences. Here the Llandovery–Wenlock is characterized by dark graptolite shales with lydite intercalations and by calcareous black shales in the Wenlock–Ludlow. Contrarily, Ludlow coarse-grained greywacke and the Upper Ludlow–Pridoli siltstone and fine-grained sandstone predominates the Upper Silurian sediments in the Kielce Region (Kozlowski 2008; Kozlowski et al. 2014; Malec 1993).

The Ludlow greywackes in the Holy Cross Mts indicate that they have a reworked continental island arc provenance (Kozlowski et al. 2014). The transport directions reflect location of this area westwardly of the Holy Cross Mts. Older sedimentary and metasedimentary rocks with high amounts of cherts and variously differentiated volcanic rocks, andesitic to dacitic in composition, were the source of detritus. The rapid deposition of the sediments, composed of immatured material, was related to turbidite sedimentation (Kozlowski 2008; Kozlowski et al. 2014).

Conglomerate-bearing coarse-grained formations are known only from the Małopolska Massif (Nida Region and Kielce Region; Malec et al. 2016; Verniers et al. 2008). In the Nida Region, the Silurian strata are composed of graptolite shale with lydite and carbonate intercalations in the Llandovery–Ludlow and siltstone, greywacke and fossil-free conglomerate (Miedziana Góra Conglomerate; Malec 1993) in the Pridoli (Moldinski and Szymanski 2001). The locally preserved conglomerate bodies are composed of clasts of Ordovician sandstones and Cambrian quartzites (Kozlowski et al. 2014). The Carpathian Foreland possibly represents the easternmost part of the Małopolska Massif and indicates a similar but more variable depositional environment to that in the Nida Region (Verniers et al. 2008). In the Kielce Region, greywackes with mudstone interbeds and conglomerates of Ludlow age above graptolite claystones are exposed in the Holy Cross Mts at Niestachów (Malec et al. 2016). Petrographic examination of Malec et al. (2016) indicates that these greywacke conglomerates and sandstones are composed of acidic–intermediate volcanic and sedimentary rock fragments, with subordinate metamorphic and scarce plutonic clasts.

In the Horváthertelend Unit, the absence of calcareous successions together with the dominance of coarse clastics

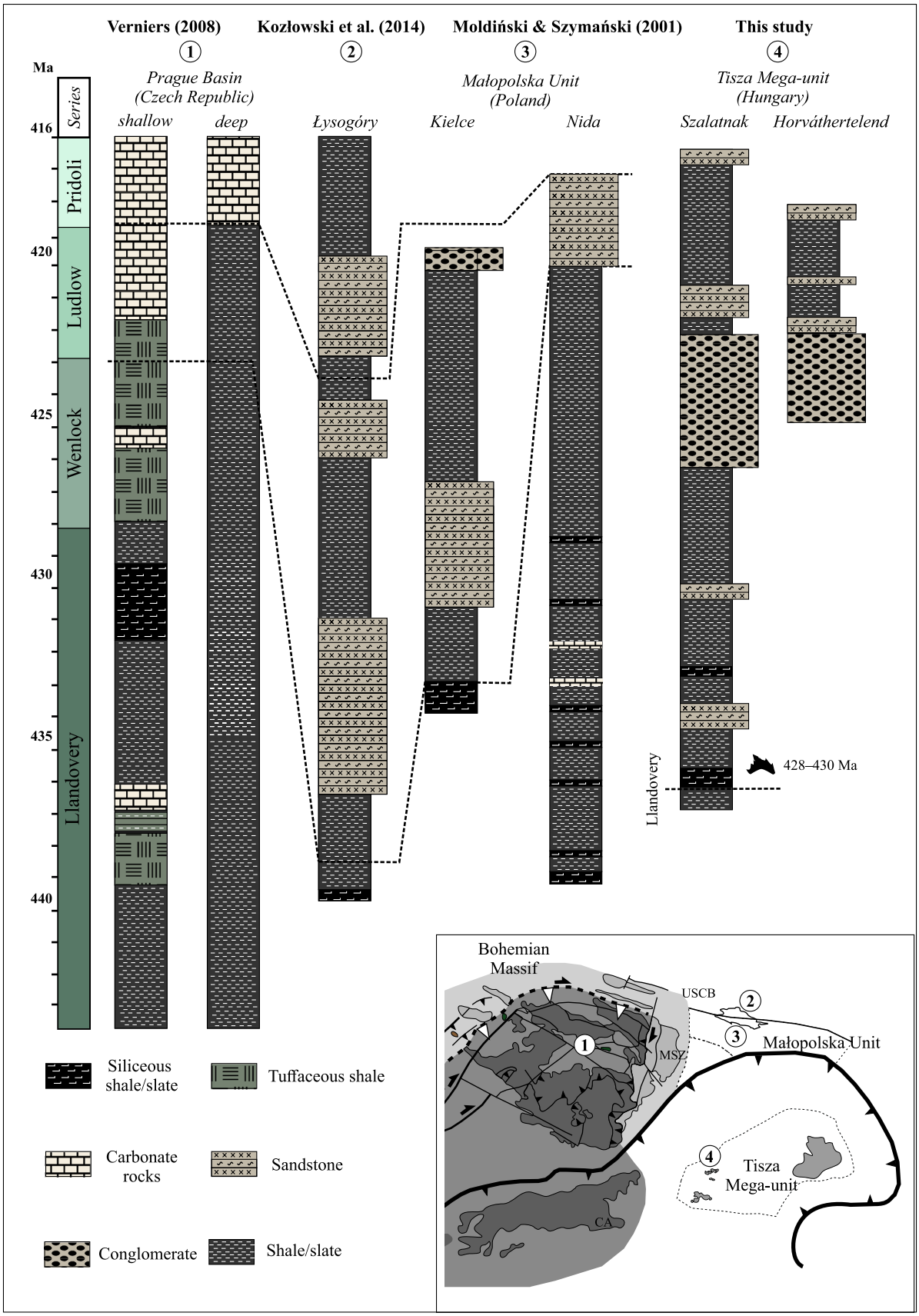
Verniers (2008)
Kozłowski et al. (2014)
Moldiński & Szymański (2001)
This study
1
2
3
4
Ma
Series
Pridoli
Ludlow
Wenlock
Llandovery
416
420
425
430
435
440
Prague Basin
(Czech Republic)
shallow
deep
Łysogóry
Małopolska Unit
(Poland)
Kielce
Nida
Tisza Mega-unit
(Hungary)
Szalatnak
Horváthertelend
Llandovery
428–430 Ma
Siliceous shale/slate
Tuffaceous shale
Carbonate rocks
Sandstone
Conglomerate
Shale/slate
Bohemian Massif
USCB
MSZ
Małopolska Unit
Tisza Mega-unit
CA

◂**Fig. 13** Main lithological features of the Silurian in the Bohemian region and in the Tisza Mega-unit (lithology after Verniers et al. 2008, Moldiński and Szymański 2001 and Kozłowski et al. 2014). CA, Carnic Alps; MSZ, Moravo-Silesian Zone; USCB, Upper Silesian Coal Basin

suggests a more proximal palaeogeographic position. The Horváthertelend metapelite samples are texturally and geochemically immature. Petrographic and geochemical features described above indicate recycled orogenic signatures with older quartz-rich sedimentary rocks and with a distinct intermediate to acidic magmatic arc component. Based on the presence of thick polymictic conglomerate intercalations with pebbles up to 20–25 cm in diameter, it can be assumed that the Silurian sediments of the Horváthertelend Unit had source areas located on the orogen side of the depositional basin.

The Szalatnak Slate Formation in the northern part of the SW Tisza Mega-unit has some remarkable similarities to the Silurian fossil-free marine, coarse clastics of the Holy Cross Mts, especially of the southern part of the Małopolska Massif near to the Upper Silesia terrane. In both depositional areas carbonate intercalations are present in subordinate amounts; additionally, these areas are predominated by proximal lithologies (greywacke, conglomerate) with geochemical signatures of active continental margin and volcanic arc tectonic settings in the upper part of the sections. In accordance with the more proximal character of the Horváthertelend foreland basin in comparison to the Kielce and Łysogóry Regions, we conclude that the Horváthertelend Unit is maybe located to the west of the Małopolska Massif (present coordinates). This reconstruction is independently confirmed by the similar framework composition of the Pennsylvanian Téseny Sandstone (SW Tisza Mega-unit) and the Cracow Sandstone (Upper Silesia) (Varga et al. 2003).

It is important to note, however, that the Silurian and the Upper Palaeozoic of the Małopolska Massif did not pass through Variscan metamorphism. The easternmost occurrence of the Variscan metamorphic Silurian and Upper Palaeozoic in the Bohemian Massif is known from the Moravo-Silesian Zone characterized by 340–320 Ma uplift ages (Dallmeyer et al. 1992; Schulmann et al. 2014; Štípská et al. 2015). In the Silesian Block of the Moravo-Silesian Zone, K-white mica K–Ar and monazite U–Th–Pb ages of 300–280 Ma are related to the post-orogenic felsic magmatism which overprinted a Barrovian type regional metamorphism reported from the NE part of the Moravo-Silesian Zone (Schulmann et al. 2014). Similar post-orogenic granodiorites with zircon U–Pb ages of ~ 300 Ma are known from the border region between the Małopolska Massif and the Upper Silesian Massif along the Kraków–Lubliniec Fault zone (Żelaźniewicz et al. 2008). The post-orogenic Variscan K–Ar ages (c. 290 Ma) of clay-size K-white mica in the Horváthertelend Unit (Tisza Mega-unit) shows very similar ages like the overprint of the post-orogenic magmatism in the NE part of Moravo-Silesian Zone and S Małopolska Massif.

Based on the lithological and geochemical features together with mica cooling ages, the Silurian Szalatnak Slate Formation of the Tisza Mega-unit seems to be referred to the Silurian of the S Małopolska Massif (Baltica) and the NE part of the Moravo-Silesian Zone.

Conclusions

The Silurian Szalatnak Slate Formation from the Horváthertelend Unit, NW part of the Tisza Mega-unit (Pannonian Basin, Hungary) consists of slates, volcanic lithic-rich metagreywackes and metaconglomerates with a combined felsic volcanic arc and recycled-orogen (e.g., quartz-rich metasediments) provenance. Both petrographic and geochemical features reflect their derivation from fractionated (mature) upper continental crust. The appearance of coarse-grained lithologies in the studied section suggests a proximal palaeogeographic position during sedimentation.

The slate samples have a highly variable mineralogical composition with a K-white mica, chlorite, quartz and albitic plagioclase assemblage together with a relatively high amount of amorphous material. The matrix of the slate has a moderately developed continuous foliation with oriented sericitic K-white mica and chlorite bands. In some cases, it associates with an anastomosing pressure solution cleavage, enriched in CM and limonite.

The K-white mica in the clay fraction has a phengitic composition and shows a strong genetic relationship with chlorite. KI_{Basel} of the K-white mica and ChC_{CIS} values of the chlorite suggest an epizonal metamorphic alteration. This is in accordance with the results of RSCM thermometry which show ~ 350–370 °C temperature for the peak metamorphism and contemporaneous ductile deformation. The 'b' cell dimension of K-white mica in the samples suggests a regional medium pressure character of the metamorphism.

The peak *T* condition is higher than the closure temperature of K-white mica so the K–Ar ages are interpreted as cooling ages. Whole rock isochron age with individual age data suggests Variscan peak metamorphism older than *c*. 310 Ma while data from the clay fraction show post-Variscan cooling ages of *c*. 290 Ma.

In accordance with the proximal character of the Silurian Horváthertelend foreland basin, we conclude that the studied Horváthertelend Unit, exotic with respect to the surrounding units in Hungary, could not belong to the Moldanubian Zone of the Bohemian Massif. The original position of this unit within the framework of the Variscan mountain chain is maybe to the northeast from the Bohemian Massif (present

coordinates), showing many similarities with the Silurian sequences of the Upper Silesian Block (Moravo-Silesian Zone) and the Małopolska Terrane (Kielce Region).

Acknowledgements Open access funding provided by University of Szeged (SZTE). We acknowledge Laurence Warr (University of Greifswald) for the CIS standards and Elemér Pál-Molnár (University of Szeged) for support of the 'Vulcano' Petrology and Geochemistry Research Group, and Félix Schubert for the helpful conversations. We thank Zoltán Máthé (Mecsekérc Ltd.) and György Szakmány (Eötvös Loránd University) and Gyöngyi Lelkesné Felvári (Hungarian Academy of Sciences) for the studied samples. We thank Tivadar M. Tóth for the support of the Department of Mineralogy, Geochemistry and Petrology. The K−Ar studies were supported by the Bolyai Research Scholarship of the Hungarian Academy of Sciences (BO/442/16) to Zsolt Benkó. The research was supported by the European Union and the State of Hungary, cofinanced by the European Regional Development Fund in the project of GINOP-2.3.2.-15-2016-00009 'ICER'. Geochemical and regional correlation studies were supported by the UNKP-17-4 New National Excellence Program of the Ministry of Human Capacities (Hungary) and the Bolyai Research Scholarship of the Hungarian Academy of Sciences (BO/266/18) to Andrea Varga. Some parts of this research was financed by the Hungarian Scientific Research Found project PD 83511 (Hungary) to Andrea Varga. We would like to thank the anonymous reviewers and Ingo Braun (topic editor) for their suggestions and comments that improve our manuscript.

Open Access This article is distributed under the terms of the Creative Commons Attribution 4.0 International License (http://creativecommons.org/licenses/by/4.0/), which permits unrestricted use, distribution, and reproduction in any medium, provided you give appropriate credit to the original author(s) and the source, provide a link to the Creative Commons license, and indicate if changes were made.

References

Aoya M, Kouketsu Y, Endo S, Shimizu H, Mizukami T, Nakamura D, Wallis S (2010) Extending the applicability of the Raman carbonaceous-material geothermometer using data from contact metamorphic rocks. J Metamorph Geol 28(9):895–914. https://doi.org/10.1111/j.1525-1314.2010.00896.x

Árkai P (1991) Chlorite crystallinity: an empirical approach and correlation with illite crystallinity, coal rank and mineral facies as exemplified by Palaeozoic and Mesozoic rocks of northeast Hungary. J Metamorph Geol 9:723–734. https://doi.org/10.1111/j.1525-1314.1991.tb00561.x

Árkai P, Cs Lantai, Lelkes-Felvári Gy, Nagy G (1995) Biotite in a Paleozoic metagreywacke complex, Mecsek Mountains, Hungary: conditions of low-T metamorphism deduced from illite and chlorite crystallinity, coal rank, white mica geobarometric and microstructural data. Acta Geol Hung 38:293–319

Árkai P, Faryad SW, Vidal O, Balogh K (2003) Very low-grade metamorphism of sedimentary rocks of the Meliata unit, Western Carpathians, Slovakia: implications of phyllosilicate characteristics. Int J Earth Sci 92:68–85. https://doi.org/10.1007/s00531-002-0303-x

Árkai P, Livi KJT, Frey M, Brukner-Wein A, Cs Sajgó (2004) White micas with mixed interlayer occupancy: a possible cause of pitfalls in applying illite Kübler index ("crystallinity") for the determination of metamorphic grade. Eur J Miner 16:469–482. https://doi.org/10.1127/0935-1221/2004/0016-0469

Balen D, Massonne HJ, Petrinec Z (2015) Collision-related Early Paleozoic evolution of a crustal fragment from the northern Gondwana margin (Slavonian Mts., Tisia Mega-Unit, Croatia): reconstruction of the P–T path, timing and paleotectonic implications. Lithos 232:211–228. https://doi.org/10.1016/j.lithos.2015.07.003

Balen D, Massonne HJ, Lihter I (2018) Alpine metamorphism of low-grade schists from the Slavonian Mountains (Croatia): new P–T and geochronological constraints. Int Geol Rev 60:288–304. https://doi.org/10.1080/00206814.2017.1328710

Balogh K (1985) K/Ar dating of Neogene volcanic activity in Hungary: Experimental technique, experiences and methods of chronologic studies. ATOMKI Rep. D/1:277–288

Beyssac O, Goffé B, Chopin C, Rouzaud N (2002) Raman spectra of carbonaceous material in metasediments: a new geo thermometer. J Metamorph Geol 20:859–871. https://doi.org/10.1046/j.1525-1314.2002.00408.x

Beyssac O, Cox SC, Vry J, Herman F (2016) Peak metamorphic temperature and thermal history of the Southern Alps (New Zealand). Tectonophysics 676:229–249. https://doi.org/10.1016/j.tecto.2015.12.024

Bhatia MR, Crook KAW (1986) Trace element characteristics of greywackes and tectonic setting discrimination of sedimentary basins. Contrib Miner Petr 92:181–193. https://doi.org/10.1007/bf00375292

Biševac V, Balogh K, Balen D, Tibljaš D (2010) Eoalpine (Cretaceous) very low- to low-grade metamorphism recorded on the illite-muscovite-rich fraction of metasediments from South Tisia (eastern Mt Papuk, Croatia). Geol Carpathica 61(6):469–481

Biševac V, Krenn E, Balen D, Finger F, Balogh K (2011) Petrographic, geochemical and geochronological investigation on granitic pebbles from Permo triassic metasediments of the Tisia terrain (eastern Papuk). Miner Petrol 102:163–180

Biševac V, Krenn E, Finger F, Lužar-Oberiter B, Balen D (2013) Provenance of Paleozoic very low- to low- grade metasedimentary rocks of South Tisia (Slavonian Mountains, Radlovac Complex, Croatia). Geol Carpathica 64(1):3–22

Buda GY, Puskás Z, Gál-Sólymos K, Klötzli U, Cousens BL (2000) Mineralogical, petrological and geochemical characteristics of crystalline rocks of Üveghuta boreholes Mórágy Hills, South Hungary). Annual Report of the Geological Institute of Hungary 1999, pp 231–252

Buda GY, Koller F, Ulrych J (2004) Petrochemistry of Variscan granitoids of Central Europe: correlation of Variscan granitoids of the Tisia and Pelsonia terranes with granitoids of the Moldanubicum, Western Carpathian and Southern Alps. A review: part I. Acta Geol Hung 47:17–138. https://doi.org/10.1556/ageol.47.2004.2-3.3

Cawood PA, Buchan C (2007) Linking accretionary orogenesis with supercontinent assembly. Earth Sci Rev 82:217–256. https://doi.org/10.1016/j.earscirev.2007.03.003

Clauer N, Chaudhuri S (1995) Clays in crustal environments. Isotopic dating and tracing. Springer Verlag Berlin, Heidelberg

Clauer N, Weh A (2014) Time constraints of the tectono-thermal evolution of the Cantabrian Zone in NW Spain by illite K-Ar dating. Tectonophysics 623:39–51. https://doi.org/10.1016/j.tecto.2014.03.013

Cox R, Lowe DR, Cullers RL (1995) The influence of sediment recycling and basement composition on evolution of mudrock chemistry in the southwestern United States. Geochim Cosmochim Ac 59:2919–2940. https://doi.org/10.1016/0016-7037(95)00185-9

Csontos L, Vörös A (2004) Mesozoic plate tectonic reconstruction of the Carpathian region. Palaeogeogr Palaeoclimatol Palaeoecol 210:1–56. https://doi.org/10.1016/j.palaeo.2004.02.033

Csontos L, Nagymarosy A, Horváth F, Kovác M (1992) Tertiary evolution of the Intra-Carpathian area: a model. Tectonophysics

208:221–241. https://doi.org/10.1016/b978-0-444-89912-5.50017-x
Csontos L, Benkovics L, Bergerat F, Mansy J, Wórum G (2002) Tertiary deformation history from seismic section study and fault analysis in a former European Tethyan margin (the Mecsek-Villány area, SW Hungary). Tectonophysics 357:81–102. https://doi.org/10.1016/s0040-1951(02)00363-3
Dallmeyer RD, Neubauer F, Höck V (1992) Chronology of late Paleozoic tectonothermal activity in the southeastern Bohemian Massif, Austria (Moldanubian and Moravo-Silesian zones): $^{40}Ar/^{39}Ar$ mineral age controls. Tectonophysics 210:135–153. https://doi.org/10.1016/0040-1951(92)90132-p
de Dunoyer Segonzac G (1970) The transformation of clay minerals during diagenesis and low-grade metamorphism: a review. Sedimentology 15:281–356. https://doi.org/10.1111/j.1365-3091.1970.tb02190.x
Erns WG (1963) Significance of phengitic micas from low-grade schist. Am Miner 48:1357–1373
Esquevin J (1969) Influence de la composition chimique des illites sur leur cristallinité. Bulletin du Centre de Recherches Pau. SNPA 3:147–153
Flinn D (1962) On folding during three-dimensional progressive deformation. Q J Geol Soc 118:385–428
Floyd EA, Leveridge BE (1987) Tectonic environment of the Devonian Gramscatho basin, south Cornwall: framework mode and geochemical evidence from turbiditic sandstones. J Geol Soc Lond 144:531–542. https://doi.org/10.1144/gsjgs.144.4.0531
Floyd EA, Winchester JA, Park RG (1989) Geochemistry and tectonic setting of Lewisian clastic metasediments from the early Eroterozoic Loch Maree Group of Gairloch, N. W Scotland. Precambrian Res 45:203–214. https://doi.org/10.1016/0301-9268(89)90040-5
Franceschelli M, Leoni L, Memmin I (1989) B_0 of muscovite in low and high variance assemblages from low grade Verrucano rocks, Northern Apennines, Italy. Schweiz Miner Petrogr Mitt 69:107–115
Frey M, Niggli E (1972) Margarite, an important rock-forming mineral in regionally metamorphosed low-grade rocks. Die Naturwissenschaften 59:214–215. https://doi.org/10.1007/bf00595509
Frey M, Robinson D (1999) Low-grade metamorphism. Blackwell Science Publishing LTD, Oxford
Fülöp J (1994) Magyarország geologiája: Paleozoikum II. Akadémiai Kiadó, Budapest **(in Hungarian)**
Glasmacher UA, Tscernoster R, Clauer N, Spaeth G (2001) K–Ar dating of magmatic sericite crystallites for determination of cooling paths of metamorphic overprints. Chem Geol 175:673–687. https://doi.org/10.1016/s0009-2541(00)00292-8
Guidotti CV, Sassi FP (1986) Classification and correlation of metamorphic facies series by means of muscovite b_0 data from low-grade metapelites. Neues Jahrbuch für Mineralogie Abhandlungen 153:363–380
Haas J, Cs Péró (2004) Mesozoic evolution of the Tisza Mega-unit. Int J Earth Sci 93:297–313. https://doi.org/10.1007/s00531-004-0384-9
Haas J, Mioč P, Pamić J, Tomljenović B, Árkai P, Bérczi-Makk A, Koroknai B, Kovács S, Felgenhauer RE (2000) Complex structural pattern of the Alpine-Dinaric-Pannonian triple junction. Int J Earth Sci 89:377–389. https://doi.org/10.1007/s005310000093
Herron MM (1988) Geochemical classification of terrigenous sands and shales from core or log data. J Sed Petrol 58:820–829. https://doi.org/10.1306/212f8e77-2b24-11d7-8648000102c1865d
Hunziker JC (1986) The evolution of illite to muscovite: an example of the behaviour of isotopes in low-grade metamorphic terrains. Chem Geol 57:31–40. https://doi.org/10.1016/0009-2541(86)90092-6
Hunziker JC, Frey M, Clauer N, Dallmeyer RD, Friedrichsen H, Flehming W, Hochstrasser K, Roggwiler P, Schwander H (1986) The evolution of illite to muscovite: mineralogical and isotopic data from the Glarus Alps, Switzerland. Contrib Miner Petr 92:157–180. https://doi.org/10.1007/bf00375291
Jamičić D (1988) Strukturni sklop slavonskih planina (Tectonics of the Slavonian Mts.) (Ph.D. Thesis), University of Zagreb; p 152. (in Croatian)
Jerenić G, Pamić J, Sremac J, Španić D (1994) Palynological and organic-petrographic data on very low- and low grade metamorphic rocks in the Slavonian Mountains (Northern Croatia). Geol Croat 47:149–155
Judik K, Rantitsch G, Rainer TM, Árkai P, Tomljenović B (2008) Alpine Metamorphism of organic matter in metasedimentary rocks from Mt. Medvednica (Croatia). Swiss J Geosci 101:605–615. https://doi.org/10.1007/s00015-008-1303-z
Kalvoda J, Babek O, Fatka O, Leichmann J, Melichar R, Nehyba S, Spacek P (2008) Brunovistulian terrane (Bohemian Massif, Central Europe) from late Proterozoic to late Paleozoic: a review. Int J Earth Sci 97:497–518. https://doi.org/10.1007/s00531-007-0183-1
Kisch HJ, Sassi R, Sassi FP (2006) The b_0 lattice parameter and chemistry of phengites from HP/LT metapelites. Eur J Miner 18:207–222. https://doi.org/10.1127/0935-1221/2006/0018-0207
Klötzli US, Gy Buda, Skiöld T (2004) Zircon typology, geochronology and whole rock Sr–Nd isotope systematics of the Mecsek Mountain granitoids in the Tisia Terrane (Hungary). Miner Petrol 81:113–134. https://doi.org/10.1007/s00710-003-0026-0
Klug HE, Alexander LE (1974) X-ray diffraction procedures. Wiley-Interscience, New York
Kouketsu Y, Mizukami T, Mori H, Endo S, Aoya M, Hara H, Nakamura D, Wallais S (2014) A new approach to develop the Raman carbonaceous material geothermometer for low-grade metamorphism using peak width. Isl Arc 23:33–50. https://doi.org/10.1111/iar.12057
Kovács G, Tóth MT, Schubert F (2009) Petrology of the Gyód serpentinite. In: Tóth MT (ed) Magmás és metamorf képződmények a Tiszai –egységben. GeoLitera, Szeged, pp 65–80 **(in Hungarian)**
Kovács G, Radovics BG, Tóth TM (2016) Petrologic comparison of the Gyód and Helesfa serpentinite bodies (Tisia Mega Unit, SW Hungary). J Geosci-czech 61:255–263. https://doi.org/10.3190/jgeosci.218
Kozłowski W (2008) Lithostratigraphy and regional significance of the Nowa Słupia Group (Upper Silurian) of the Łysogóry Region (Holy Cross Mountains, Central Poland). Acta Geol Pol 58:43–74
Kozłowski W, Domańska-Siuda J, Nawrocki J (2014) Geochemistry and petrology of the Upper Silurian greywackes from the Holy Cross Mountains (central Poland): implications for the Caledonian history of the southern part of the Trans-European Suture Zone (TESZ). Geol Q 58:311–336. https://doi.org/10.7306/gq.1160
Kozur H (1984) Muellerisphaerida eine neue Ordnung von Mikrofossilien unbekannter systematischer Stellung aus dem Silur und Unterdevon von Ungarn. Geologisch-Paläontologische Mitteilungen Innsbruck 13:125–148
Kříbek B, Žák K, Dobeš P, Leichmann J, Pudilová M, René M, Scharm B, Scharmová M, Hájek A, Holeczy D, Hein UF, Leichmann B (2009) The Rožná uranium deposit (Bohemian Massif, Czech Republic): shear zone-hosted, late Variscan and post-Variscan hydrothermal mineralization. Miner Depisota 44:99–128. https://doi.org/10.1007/s00126-008-0188-0
Kroner U, Mansy J-L, Mazur S, Aleksandrowski P, Hann HP, Huckriede H, Lacquement F, Lamarche J, Ledru P, Pharaoh TC, Zedler H, Zeh A, Zulauf G (2008) Variscan tectonics. In: McCann T (ed) The Geology of Central Europe, precambrian and palaeozoic. Geol Soc Lond, London

Kübler B (1964) Les argiles, indicateurs de métamorphisme. Revue Institute de la Française de Pétrole 19:1093–1112
Kübler B (1967) La cristallinité de l'illite et les zones tout à fait supérieures de métamorphisme. In: Schaer JP (1967). Colloque sur les étages tectoniques, À la Baconnière, Neuchâtel, pp 105–122
Kübler B, Jaboyedoff M (2000) Illite crystallinity. Earth Planet Sc Lett 331:75–89. https://doi.org/10.1016/s1251-8050(00)01395-1
Lahfid A, Beyssac O, Deville E, Negro F, Chopin C, Goffé B (2010) Evolution of the Raman spectrum of carbonaceous material in low-grade metasediments of the Glarus Alps (Switzerland). Terra Nova 22:354–360. https://doi.org/10.1111/j.1365-3121.2010.00956.x
Leitch EC, McDougall I (1979) The age of orogenesis in the Nambucca Slate Belt: a K–Ar study of low-grade regional metamorphic rocks. J Geol Soc Aust 26:111–119. https://doi.org/10.1080/00167617908729074
Livi KJT, Veblen DR, Ferry JM, Frey M (1997) Evolution of 2:1 layered silicates in low-grade metamorphosed Liassic shales of Central Switzerland. J Metamorph Geol 15:323–344. https://doi.org/10.1111/j.1525-1314.1997.00019.x
Lünsdorf NK (2016) Raman spectroscopy of dispersed vitrinite—Methodical aspects and correlation with reflectance. Int J Coal Geol 153:75–86
Lünsdorf NK, Dunkl I, Schmidt BC, Rantitsch G, von Eynatten H (2014) Towards a higher comparability of geothermometric data obtained by Raman spectroscopy of carbonaceous material. Part I: evaluation of biasing factors. Geostand Geoanalyt Res. 38:73–94
Lünsdorf NK, Dunkl I, Schmidt BC, Rantitsch G, von Eynatten H (2017) Towards a higher comparability of geothermometric data obtained by Raman spectroscopy of carbonaceous material. Part 2: a revised geothermometer. Geostand Geoanalyt Res. 41:593–612
Malec J (1993) Upper silurian and lower devonian in the western Holy Cross Mts. Geol Q 37:501–536
Malec J, Kuleta M, Migaszewski ZM (2016) Lithologic-Petrographic characterization of Silurian rocks in the Niestaców profile (Holy Cross Mountains). Annales Societatis Geologorum Poloniae 86:85–110. https://doi.org/10.14241/asgp.2015.017
Massonne H-J, Schreyer W (1987) Phengite geobarometry based on the limiting assemblage with K-feldspar, phlogopite, and quartz. Contrib Miner Petr 96:212–224. https://doi.org/10.1007/bf00375235
Massonne H-J, Szpurka Z (1997) Thermodynamic properties of white micas on the basis of high-pressure experiments in the systems K_2O–MgO–Al_2O_3–SiO_2–H_2O and K_2O–FeO–Al_2O_3–SiO_2–H_2O. Lithos 41:229–250
McLennan SM (1989) Rare earth elements in sedimentary rocks: influence of provenance and sedimentary processes. In: Lipin BR, Mcka YGA, editors. Geochemistry and mineralogy of rare earth elements. Reviews in Mineralogy, 21:169–200
Merriman RJ, Roberts B, Peacor DR (1990) A transmission electron microscope study of white mica crystallite size distribution in mudstone to slate transitional sequence, North Wales, UK. Contrib Miner Petr 106:27–40. https://doi.org/10.1007/bf00306406
Mészáros E, Raucsik B, Varga A, Schubert F (2016) Low-grade, medium pressure regional metamorphism of the pelitic succession in the borehole Horváthertelend Hh-1: microstructural and thermobarometric evidences. Földtani Közlöny (In Hungarian with English abstract) 146:207–222
Miyashiro A (1994) Metamorphic petrology. UCL Press, London
Moldiński Z, Szymański B (2001) The Silurian of the Nida, Holy Cross Mts. and Radom areas, Poland—a review. Geol Q 45:35–454
Mori H, Mori N, Wallis S, Westaway R, Annen C (2016) The importance of heating duration for Raman CM thermometry: evidence from contact metamorphism around the Great Whin Sill intrusion, UK. J Metamorph Geol 35:165–180. https://doi.org/10.1111/jmg.12225
Nier AO (1950) A redetermination of the relative abundances of the isotopes of carbon, nitrogen, oxygen, argon and potassium. Physl Rev Lett 77:789–793
Novo-Fernández I, Garcia-Casco A, Arenas R, Diéz Fernaández R (2016) The metahyaloclastitic matrix of a unique metavolcanic block reveals subduction in the Somozas Mélange (Cabo Ortegal Complex, NW Iberia): tectonic implications for the assembly of Pangea. J Metamorph Geol 34:963–985. https://doi.org/10.1111/jmg.12216
Oravecz J (1964) Szilur képződmények Magyarországon. Földtani Közlöny 94:3–9 **(in Hungarian)**
Padan A, Kisch HJ, Shagam R (1982) Use of the lattice parameter b_0 of dioctahedral illite/muscovite for the characterization of P/T gradients of incipient metamorphism. Contrib Miner Petr 79:85–95. https://doi.org/10.1007/bf00376965
Pamić J, Jamičić D (1986) Metabasic intrusive rocks from the Paleozoic Radlovac complex of Mt. Papuk in Slavonija (northern Croatia). Rad Jugoslavenske Akademije Znanosti Umjetnosti Zagreb 424:97–125
Pamić J, Tomljenović B (1998) Basic geologic data from the Croatian part of the Zagorje–Mid-Transdanubian Zone. Acta Geol Hung 41:389–400
Paschier CW, Trouw RAJ (2005) Microtectonics. Springer-Verlag, Berlin, Heidelberg
Pettijohn FJ, Potter PE, Siever R (1972) Sand and sandstone. Springer-Verlag, New York
Rahl J, Anderson K, Brandon M, Fassoulas C (2005) Raman spectroscopic carbonaceous material thermometry of low-grade metamorphic rocks: calibration and application to tectonic exhumation in Crete, Greece. Earth Planet Sc Lett 240(2):339–354. https://doi.org/10.1016/j.epsl.2005.09.055
Ramsey JG, Huber MI (1983) The techniques of modern structural geology I: strain. Academy Press, London
Rantitsch G, Judik K (2009) Alpine metamorphism in the central segment of the Western Greywacke Zone (Eastern Alps). Geol Carpath 60:319–329. https://doi.org/10.2478/v10096-009-0023-2
Sassi FP (1972) The petrological and geological significance of the b_0 velues of the potassic white micas in low-grade metamorphic rocks. An application to the Eastern Alps. Tschermaks mineralogische und petrographische Mitteilungen, 18/2:105–113
Sassi FP, Scolari A (1974) The b_0 value of the potassic white micas as a barometric indicator in low-grade metamorphism of pelitic schists. Contrib Miner Petr 45:143–152. https://doi.org/10.1007/bf00371166
Schmid SM, Bernoulli D, Fügenschuh B, Matenco L, Schefer S, Schuster R, Tischler M, Ustaszewski K (2008) The Alpine-Carpathian-Dinaric orogenic system: correlation and evolution of tectonic units. Swiss J Geosci 101:139–183. https://doi.org/10.1007/s00015-008-1247-3
Schulmann K, Oliot E, Košuličová M, Montigny R, Štípská P (2014) Variscan thermal overprint exemplified by U–Th–Pb monazite and K–Ar muscovite and biotite dating at the eastern margin oft he Bohemian Massif (East Sudetes, Czech Republic). J Geosciczech 59:389–413. https://doi.org/10.3190/jgeosci.180
Shafiqullah M, Damon PE (1974) Evaluation of K–Ar isochron methods. Geochim Cosmochim Ac 38:1341–1358. https://doi.org/10.1016/0016-7037(74)90092-1
Steiger RH, Jäger E (1977) Subcommission on geochronology: convention on the use of decay constants in geo- and cosmochronology. Earth Planet Sci Lett 12:359–362. https://doi.org/10.1016/0012-821x(77)90060-7
Stipp M, Kunze K (2008) Dynamic recrystallization near the brittle-plastic transition in naturally and experimentally deformed quartz

aggregates. Tectonophysics 448:77–97. https://doi.org/10.1016/s0191-8141(02)00035-4

Stipp M, Stünitz H, Heilbronner R, Schmid SM (2002) The eastern Tonale fault zone: a 'natural laboratory' for crystal plastic deformation of quartz over a temperature range from 250 to 700 °C. J Struct Geol 24:1861–1884. https://doi.org/10.1016/s0191-8141(02)00035-4

Štípská P, Hacker BR, Racek M, Holder R, Kylander-Clark ARC, Schulmann K, Haslová P (2015) Monazite dating of prograde and retrograde P–T-d paths in the Barrovian terrane oft he Thaya window, Bohemian Massif. J Petrol 56:1007–1035. https://doi.org/10.1093/petrology/egv026

Štorch P (1999) Upper Ordovician—Lower Silurian sequences of the Bohemian Massif, central Europe. Geol Mag 127:225–239

Štroch P, Kraft P (2009) Graptolite assemblages and stratigraphy of the lower Silurian Mrákotín Formation, Hlinsko Zone, NE interior of the Bohemian Massif (Czech Republic). Bull Geosci 84:51–74. https://doi.org/10.3140/bull.geosci.1077

Suchý V, Sýkorová I, Stejskal M, Šafanda J, Michovič V, Novotná M (2002) Dispersed organic matter from Silurian shales of the Barrandian Basin, Czech Republic: optical properties, chemical composition and thermal maturity. Int J Coal Geol 53:1–25. https://doi.org/10.1016/s0140-6701(03)81625-9

Suchý V, Sandler A, Slobodník M, Sýkorová I, Filip J, Melka K, Zeman A (2015) Diagenesis to very low-grade metamorphism in lower Palaeozoic sediments: a case study from deep borehole Tobolka 1, the Barrandian Basin, Czech Republic. Int J Coal Geol 140:41–62. https://doi.org/10.1016/j.coal.2014.12.015

Szederkényi T (1996) Metamorphic formations and their correlation in the Hungarian part of Tisia Megaunit (Tisia Megaunit Terrane). Acta Miner Petrogr 37:143–161

Szederkényi T, Haas J, Nagymarosy A, Hámor G (2012) Geology and history of evolution of Tisza Mega-Unit. In: Haas J (ed) Geology of Hungary. Springer Verlag, Berlin

Taylor SR, Mclennan SM (1985) The Continental Crust: its Composition and Evolution. Blackwell Scientific Publications LTD, Oxford

Varga A, Gy Szakmány, Máthé Z, Józsa S (2003) Petrology and geochemistry of Upper Carboniferous siliciclastic rocks (Téseny Sandstone Formation) from the Slavonian-Drava Unit (Tisza Megaunit, S Hungary)—summarised results. Acta Geol Hung 46:95–113

Varga A, Szakmány Gy, Árgyelán T, Józsa S, Raucsik B, Máthé Z (2007) Complex examination of the Upper Paleozoic siliciclastic rocks from southern Transdanubia, SW Hungary—Mineralogical, petrographic, and geochemical study. In: Arribas J, Critelli S, Johnsson MJ, editors. Sedimentary Provenance and Petrogenesis: Perspectives from Petrography and Geochemistry. Geological Society of America Special Paper 420:221–240. https://doi.org/10.1130/2006.2420(14)

Velde B (1965) Phengite micas: synthesis, stability and natural occurrence. Am J Sci 263:886–913. https://doi.org/10.2475/ajs.263.10.886

Verniers J, Maletz J, Kříž J, Žigaitė Ž, Paris F, Schönlaub HP, Wrona R (2008) Silurian. In: McCann T (ed) The Geology of Central Europe: Precambrian and Palaeozoic. Geological Society of London, London, pp 299–302

von Raumer JF, Stampfli GM, Bussy F (2003) Gondwana-derived microcontinents—the constituents of the Variscan and Alpine collisional orogens. Tectonoshysics 365:7–22. https://doi.org/10.1016/s0040-1951(03)00015-5

Vozár J, Ebner F, Vozárová A, Haas J, Kovács S, Sudar M, Bielik M, Cs Péró (2010) Variscan and Alpine terranes of the Circum-Pannonian Region. Slovak Academy of Sciences, Geological Institute, Bratislava

Warr LN, Mählmann RF (2015) Recommendations for Kübler Index standardization. Clay Miner 50:282–285. https://doi.org/10.1180/claymin.2015.050.3.02

Warr LN, Rice AHN (1994) Interlaboratory standardization and calibration of clay mineral crystallinity and crystallite size data. J Metamorph Geol 12:141–152. https://doi.org/10.1111/j.1525-1314.1994.tb00010.x

Whitney DL, Evans BW (2010) Abbreviation for names of rock-forming minerals. Am Miner 95:185–187. https://doi.org/10.2138/am.2010.3371

Wiederkehr M, Bousquet R, Ziemann MA, Berger A, Schmid SM (2011) 3-D assessment of peak-metamorphic conditions by Raman spectroscopy of carbonaceous material: an example from the margin of the Lepontine dome (Swiss Central Alps). Int J Earth Sci 100:1029–1063. https://doi.org/10.1007/s00531-010-0622-2

Yui TF, Huang E, Xu J (1996) Raman spectrum of carbonaceous material: a possible metamorphic grade indicator for low-grade metamorphic rocks. J Metamorph Geol 14:115–124. https://doi.org/10.1046/j.1525-1314.1996.05792.x

Żelaźniewicz A, Pańczyk M, Nawrocki J, Fanning M (2008) A Caboniferous/Permian, calc-alkaline, I-type granodiorite from the Małopolska Block, Southern Poland: implications from geochemical and U-Pb zircon age data. Geol Q 52:301–308